Tectonic interleaving along the Main Central Thrust, Sikkim Himalaya

Tectonic interleaving along the Main Central Thrust, Sikkim Himalaya

Catherine M. Mottram[1*], T.W. Argles[1], N.B.W. Harris[1], R.R. Parrish[2,3], M.S.A. Horstwood[3], C.J. Warren[1], S.Gupta[4]

[1]Department of Environment, Earth and Ecosystems, Centre for Earth, Planetary, Space and Astronomical Research (CEPSAR), The Open University, Walton Hall, Milton Keynes, MK7 6AA, United Kingdom
[2] Department of Geology, University of Leicester, University road, Leicester, LE1 7RH, United Kingdom
[3] NERC Isotope Geosciences Laboratory, British Geological Survey, Keyworth, Nottingham NG12 5GG, United Kingdom
[4] Department of Geology & Geophysics, I.I.T., Kharagpur – 721 302, India.
* corresponding author (e-mail: catherine.mottram@open.ac.uk)

Number of words of abstract (194), text (6,127), references (3,216), and figures (569) = **10,106 words**

Abbreviated title: Tectonic interleaving along the MCT

Abstract

Geochemical and geochronological analyses provide quantitative evidence about the origin, development and motion along ductile faults, where kinematic structures have been overprinted. The Main Central thrust (MCT) is a key structure in the Himalaya that accommodated substantial amounts of the India-Asia convergence. This structure juxtaposes two isotopically distinct rock packages across a zone of ductile deformation. Structural analysis, whole-rock Nd isotopes, and U-Pb zircon geochronology reveal that the hanging wall is characterised by detrital zircon peaks at ~800-1000 Ma, 1500-1700 Ma and 2300-2500 Ma, an $\varepsilon Nd_{(0)}$ signature of -18.3 to -12.1, and is intruded by ~800 Ma and ~500-600 Ma granites. In contrast, the footwall has a prominent detrital zircon peak at ~1800-1900 Ma, with older populations spanning 1900-3600 Ma, and an $\varepsilon Nd_{(0)}$ signature of -27.7 to -23.4, intruded by ~1830 Ma granites.

The data reveal a ~5 km thick zone of tectonic imbrication, where isotopically out-of-sequence packages are interleaved. The rocks became imbricated as the once proximal and distal rocks of the Indian margin were juxtaposed by Cenozoic movement along the MCT. Geochronological and isotopic characterisation allows for correlation along the Himalayan orogen and could be applied to other cryptic ductile shear zones.

Key words: Himalayan Geology, Geochemistry, Geochronology, Main Central thrust, Sikkim

Supplementary material: table of zircon U-Pb geochronological data, table of whole-rock Sm-Nd isotopic data, (S1) table of sample locations, (S2) photomicrographs of sample thin sections, (S3) atlas of zircon cathodoluminescence images, and (S4-6) detailed analytical conditions are available online at www.geolsoc.org.uk/SUPxx.

Crustal thickening in major orogenic belts is often achieved by packages of rock being thrust upon one another along major thrust faults. At depth, thrust faults form ductile shear zones and the amount of displacement along these structures is probably much larger than can be evaluated by strain analysis of the exposed rock. The Sikkim Himalaya provides a uniquely preserved window into the mid-crustal levels of one of the largest ductile shear zones on Earth. This study illustrates how isotope geochemistry and geochronology can be used to investigate major orogenic structures, affected by hundreds of kilometres of relative displacement and ductile deformation, to provide a unique perspective on the hanging wall-footwall relationships.

The Main Central thrust (MCT) is an orogen-parallel ductile thrust fault or shear zone that separates the Greater Himalayan Sequence (GHS) in the hanging wall from the Lesser Himalayan Sequence (LHS) in the footwall (Fig. 1; Heim and Gansser 1939; Le Fort 1975). Despite this simple definition, in reality the specific location and structural characteristics of the MCT have long been subject to debate throughout the Himalaya. Our knowledge of this thrust system in the eastern Himalaya is particularly poor.

The MCT was originally mapped in the Kumaun region of NW India as the basal contact between the crystalline nappes (GHS) and the underlying metasedimentary rocks (LHS) (Heim and Gansser 1939). Since this time there has been little agreement on the classification or location of the thrust in many Himalayan sections. A variety of factors have caused controversy over the MCT: the divergent criteria used to define the thrust, differences in methods and approach, and variations in appearance of the thrust in the field (Searle et al. 2008 and references therein). Different criteria used to define the thrust include: i) lithological changes (Heim and Gansser 1939; Valdiya 1980;

Gansser 1983; Pêcher 1989; Davidson et al. 1997; Daniel et al. 2003; Tobgay et al. 2012); ii) high strain in a distinct zone (Stephenson et al. 2001; Gupta et al. 2010); iii) metamorphic discontinuities (Bordet 1961; Le Fort 1975; Hubbard and Harrison 1989; Stäubli 1989; Harrison et al. 1997; Catlos et al. 2001; Kohn et al. 2001; Daniel et al. 2003; Groppo et al. 2009; Martin et al. 2010); iv) structural criteria (Pêcher 1989; Martin et al. 2005; Searle et al. 2008); and v) isotopic breaks (Inger and Harris 1993; Parrish and Hodges 1996; Whittington et al. 1999; Ahmad et al. 2000; Robinson et al. 2001; Martin et al. 2005; Richards et al. 2005; Richards et al. 2006; Ameen et al. 2007; Imayama and Arita 2008; Gehrels et al. 2011; Long et al. 2011b; Martin et al. 2011; Tobgay et al. 2011; McQuarrie et al. 2013; Webb et al. 2013).

It has been asserted that "the essential criteria to define a shear zone are the identification of a strain gradient and the clear localisation of strain" (Passchier and Trouw 2005, p. 532; Searle et al., 2008). Although this approach is useful to define the MCT in areas where structural criteria are clear-cut, it does not take into account the diffuse nature of the deformation that is associated with the MCT in many other transects. This approach also fails to address the difficulties of locating the thrust as a discrete break, when it separates rocks of very similar lithologies over a wide zone of ductile deformation, where total strain may not be faithfully recorded by all lithologies.

In areas where the structural and stratigraphic criteria are ambiguous, geochemical fingerprinting can potentially provide a complementary tool to identify and investigate the tectono-stratigraphic break across the MCT, as units either side of the MCT are defined by distinct geochemical signatures. Early studies found that the 'geochemical' boundary associated with the MCT coincided with the geological/lithological boundary mapped by others, suggesting that the approach had broad validity in confirming the location of the suspected major fault (e.g. Parrish and Hodges 1996). Most of these previous isotopic studies used to identify the location of the MCT have largely focused on the central and western Himalaya (see references above). More recently the eastern Himalaya have become a focus of interest for using isotopic methods (Tobgay et al. 2011; McQuarrie et al. 2013) after

suggestions that the provenance of these rocks differs from elsewhere along the orogen (Yin et al. 2010a; Yin et al. 2010b; Webb et al. 2013). Our study aims to extend the Himalayan isotopic dataset into the eastern Himalaya to allow for cross-correlation of units along the entire orogen and to assess the robustness of the isotopic approach for defining structures across thousands of kilometres of their length along strike.

Here we use lithological, structural and geochemical data to characterise the lithotectonic units of the Sikkim Himalaya, a region that lies between the well-studied regions of Nepal and Bhutan. We demonstrate, for the first time, an isotopic method of defining the location of the MCT in the Sikkim Himalaya. The data show there is a break in the geochemical signature of the rocks towards the top of the MCT zone, indicating that the deformation has penetrated down into the 'footwall' of the isotopic discontinuity. In detail, there is a zone of tectonic interleaving in the highest structural levels of the high-strain zone, which implies that tectonic imbrication in the ductile MCT zone accompanied thrusting. A model is presented outlining the provenance of these rocks and how they were juxtaposed during Cenozoic movement of the MCT. Our study permits correlation between the MCT in the Sikkim Himalaya and the MCT mapped along strike in the central and western Himalaya using a combined set of comparable data.

Geological setting

The MCT broadly represents a protolith boundary that divides two lithological packages, each characterised by distinctive geochronological and geochemical signatures (e.g. Parrish and Hodges 1996). The LHS is a Palaeoproterozoic metasedimentary sequence with an $\varepsilon Nd_{(0)}$ signature of -20 to -25 that has been intruded by ~1.8 Ga granites. In contrast, the GHS is a younger, Neoproterozoic-Ediacaran (and possibly Palaeozoic) sequence of metasedimentary rocks, characterised by an $\varepsilon Nd_{(0)}$ signature of -15 to -20 indicative of younger source regions, typically intruded by younger, ~500 and subordinate ~830 Ma granites (Parrish and Hodges 1996; Ahmad et al. 2000; Robinson et al. 2001;

Martin et al. 2005; Richards et al. 2005; Imayama and Arita 2008; Gehrels et al. 2011; Long et al. 2011b; Martin et al. 2011; Tobgay et al. 2011; McQuarrie et al. 2013; Webb et al. 2013).

In southern Sikkim and the Darjeeling Hills (referred to collectively as the Sikkim Himalaya) a combination of poor exposure around the MCT and widespread diffuse ductile deformation obscure both the location and nature of the MCT. Previous studies have identified a zone, up to 20 km wide (in map view), of ductile deformation and inverted metamorphism termed the Main Central thrust 'Zone' (Goswami 2005; Gupta et al. 2010; Fig. 2a). Although this inverted metamorphic sequence is recognised elsewhere along the Himalaya, there are few other localities where there is such a well-developed and complete sequence of Barrovian metamorphic zones (Dasgupta et al. 2009), from the biotite-in isograd to the second sillimanite-in zone (Fig. 2b and see photomicrographs in the supplementary material S2 for metamorphic minerals). A late-stage duplex beneath the Ramgarh thrust (Bhattacharyya and Mitra 2009; Long et al. 2011a) has created the Teesta Dome, deforming the MCT and producing one of the largest re-entrants, in map view, across the Himalaya (Figs 2a, 2c). Throughout the region, the MCT separates the overlying GHS from the LHS. The transition between these two rock packages in this ductile shear zone appears gradational in various respects. There is a several kilometre-wide zone of penetratively deformed rocks, with no obvious single discrete horizon of much higher strain located within this wide zone. Structurally lower levels of the zone consist of pelitic schists, psammites, quartzites, calc-silicates and orthogneisses known locally as the Lingtse gneiss (Paul et al. 1982). Sequences of paragneiss, orthogneiss and migmatites become increasingly abundant in the overlying, highest-grade rocks, but there is no single, abrupt change from one lithology to another. The inverted metamorphic zones appear continuous over a very wide extent, up to 50km across strike, and this gradual change in peak P-T conditions lacks a single discrete discontinuity in grade at any level in the zone. The apparent absence of a zone of this width elsewhere in the Himalaya may result from later brittle movement on the MCT that has truncated the zone of earlier ductile deformation in these transects (Macfarlane et al. 1992).

In the Sikkim Himalaya, there have been many conflicting interpretations of the exact location of the MCT. Studies have variously bounded the MCT zone with two named thrusts (Catlos et al. 2004; Dubey et al. 2005; Bhattacharyya and Mitra 2009; 2011), placed the MCT at the top of the MCT zone (Ghosh 1956; Acharyya 1975; Banerjee et al. 1983) or placed the MCT at the base of the MCT zone (Searle and Szulc 2005). Furthermore, the distinctive Palaeoproterozoic Lingtse gneiss, strongly sheared along the MCT zone throughout the Sikkim Himalaya, has been used in other studies as a defining lithology for determining the location of the MCT (Neogi et al. 1998; Chakraborty et al. 2003; Dasgupta et al. 2004).

We have collected both structural measurements and samples along several transects across the MCT in the Sikkim Himalaya (Fig. 2b). Throughout the region, the MCT zone displays well-developed, polydeformational fabrics typical of large-scale shearing and thrusting that have been extensively described and catalogued in previous structural studies (Goswami 2005). Structures are dominated by south-directed thrusting along the MCT as typified by the Mangan transect with fabrics detailed in Figure 3. There is a strong N-S stretching lineation identified from boudinage structures (Fig. 3a), stretching fabrics in L-tectonites (Fig. 3b), aligned fold axes, and mineral lineations (Fig. 3d). Extensive shearing has formed the main penetrative MCT foliation. Shearing is also localised into well-developed shear bands in metapelites (Fig. 3c) across several kilometres of thickness of the MCT zone. Shear indicators indicate a top-to-the-south sense of shear.

Structural mapping reveals that there are high-strain indicators distributed over a distance of ~20 km across and beneath the MCT (Fig. 3); hence most previous studies have considered the MCT to form a ‘zone’. The rocks within this zone differ in strength and rheology, creating several domains of high strain. The MCT cannot be marked or mapped as a single plane within this zone due to the distributed nature of the strain. This is illustrated in the Mangan section (Fig. 3) where the strain appears to be recorded differently in each lithology. In the metapelites, strain is localised into shear bands, whereas early quartz veins are boudinaged and the mechanically strong orthogneisses

develop L-tectonite and LS-tectonite fabrics. The deformation associated with the MCT is principally syn-metamorphic with earlier strain fabrics being reworked and/or erased by metamorphic recrystallization and new mineral growth.

In summary, the widespread, heterogeneous and diffuse nature of the strain associated with the MCT zone in the Sikkim Himalaya obscures the differentiation between the LHS and GHS purely on the basis of lithology and/or deformation. This has prompted this study into the use of geochemical and geochronological data in addressing the problem of understanding the location and nature of the MCT.

Analytical methods

Zircon U-Pb geochronology

Samples for zircon U-Pb geochronology were collected from clastic metasedimentary and igneous protoliths across the MCT in the Sikkim Himalaya to investigate the tectonic affinity of these rocks (locations shown in Fig. 2b, and in the table and photomicrographs in the supplementary material S1 and S2). Thirteen samples were collected: six quartzites for detrital zircon analysis and seven orthogneiss samples, representing pre-Himalayan granites metamorphosed during the Tertiary orogeny.

Zircon was analysed using laser ablation multi-collector inductively-coupled plasma mass spectrometry (LA-MC-ICP-MS) at the NERC Isotope Geosciences Laboratory, Keyworth, UK. Separated grains were imaged using cathodoluminescence scanning electron microscopy (SEMCL), on a FEI Quanta 600 ESEM, at 10nA, 15mm working distance at the British Geological Survey, UK to investigate zoning patterns and to choose appropriate spots for analysis (see CL images in the supplementary material S3). The zircons show several stages of growth recorded in the concentric zoning patterns of the magmatic crystals. Some zircons had more complex histories due to additional

post-magmatic metamorphic growth (see the supplementary material S3 for atlas of zircon textures).

Zircons were mainly analysed for U-Pb isotopes using a Nu Plasma HR multi-collector inductively coupled plasma mass spectrometer (MC-ICP-MS) (Nu Instruments, Wrexham, UK) and a UP193FX (193nm) excimer or UP193SS (193nm) Nd:YAG laser ablation system (New Wave Research, UK). Measurement procedures followed methods described in Thomas et al. (2010) and full analytical conditions are given in the supplementary material S4. A small number of zircons (sample 292) were analysed using an AttoM single collector sector field (SC-SF) ICP-MS (Nu Instruments, Wrexham, UK) and a New Wave Research UP193FX (193nm), excimer ablation system (New Wave Research, UK). The instrumental configuration and measurement procedures follow previous methods (Thomas et al. 2013) and full analytical conditions are shown in the supplementary material S5. Only $^{206}Pb/^{238}U$ data within 5% of concordance were plotted in relative probability plots in Figures 6 and 7. Between eighty and one hundred grains were analysed for each sample in order to retain statistically significant numbers of concordant analyses. For this number of grains, it has been calculated by Vermeesch (2004) that no fraction of the population comprising more than 5.7-6.8% of the total is missed at the 95% confidence level. All data, quoted at 2σ confidence level, are shown in the U-Pb data table in the supplementary material.

Sm-Nd Geochemistry

Twenty samples for whole-rock Nd geochemistry were collected along transects across the MCT in the Sikkim Himalaya. Schistose pelitic samples (rather than more psammitic samples) were selected because of their high REE concentration and because their fine-grained sedimentary protoliths present a more representative average of the source region (McLennan et al. 1989). Full sample locations and rock types are shown on map in Fig. 2b and in the Sm–Nd whole rock data table, and photomicrographs in the supplementary material S2.

Nd isotope analyses were obtained at The Open University, UK, by thermal ionisation mass spectrometry (TIMS) using a Triton instrument. Isotopic analytical techniques are as described by Pin and Zalduegui (1997). Full details of sample preparation and analytical conditions can be found in the supplementary material S6. $^{147}Sm/^{144}Nd$ ratios were calculated from elemental ratios obtained from quadrupole ICP-MS (full conditions in the supplementary material S6). Epsilon Nd values were calculated at time 0 using present day CHUR values of 0.512638 (Hamilton et al. 1983).

Results

Orthogneiss geochronology

The ages of the analysed zircons from the seven orthogneiss samples (Figs 4, 5 and 8) fall into three age groups; Palaeoproterozoic granites (Lingtse gneiss), Neoproterozoic granites, and Ediacaran-Cambrian granites. Each of these samples yield discordant scattered age populations due to the later metamorphism and subsequent Pb loss which affected these zircons. Ages have therefore been reported as average $^{207}Pb/^{206}Pb$ ages with 2SD uncertainties. Lingtse gneiss (samples 49 and 58) from the same body of granitic gneiss, yield average $^{207}Pb/^{206}Pb$ ages within error of each other (Sample 49= 1837 ± 45 Ma, MSWD 11.6 and Sample 58= 1836 ± 26 Ma, MSWD 11.5). Samples 233 and 245 are from two thin Lingtse gneiss units interlayered with metasedimentary rocks and record average $^{207}Pb/^{206}Pb$ ages of 1834 ± 37 Ma, MSWD 20 (Sample 233) and 1853 ± 19 Ma, MSWD 17 (Sample 245). These ages are interpreted as the timing of magmatic intrusion of the granite pluton as the analyses are yielded from zircons with typical magmatic oscillatory zoning (see zircon atlas in the supplementary material S3). All of the Lingtse gneiss samples contain older zircon cores that preserve evidence of older Proterozoic and Archaean magmatic events.

The three analysed Neoproterozoic and Ediacaran orthogneiss samples record three separate magmatic events (Fig. 5). Although all the samples contain inherited zircon cores that match the Palaeoproterozoic age of the Lingtse gneiss, the main magmatic zircon populations of these granites

vary in age. The youngest sample (280) yields a spread in age of ~490 – 520 Ma, which produced an average $^{207}Pb/^{206}Pb$ age of 508 ± 22 Ma (MSWD=3.3); sample 115 yields an average $^{207}Pb/^{206}Pb$ age of 604 ± 28 Ma (MSWD=7); and the oldest sample (32) yields an average $^{207}Pb/^{206}Pb$ age of 829 ± 28 Ma (MSWD=16).

Detrital zircon geochronology

The detrital zircon data from the six samples analysed are presented in Figures 6, 7 and 8. Four of the samples yield detrital zircon populations that have a prominent peak at ~1800 Ma with older grains spread throughout the Proterozoic and Archaean, and yield no grains younger than ~1700 Ma. In detail, samples 12 and 38x show dominant 1800 Ma peaks with a small number of older zircons. Sample 203 shows a peak at ~1900 Ma and relatively more Archaean zircons than samples 12 and 38x. Sample 292 lacks a dominant peak but zircon ages range from ~1900 Ma to ~2600 Ma; this sample contains the oldest zircons seen in this study, dating to c.3600 Ma. The remaining two samples (161 and 211) also contain minor components of Proterozoic and Archaean material, but display a range of ages down to younger than ~800 Ma. Sample 161 yields a dominant age peak at ~800-1100 Ma with minor, older, peaks at ~1500-1700 Ma and ~2300-2500 Ma. Sample 211 yields a similar age spectrum, but with a slightly older dominant peak at ~1000-1300 Ma and a spread of older zircons from 1300 Ma to 2600 Ma. There is also one discordant zircon analysis at ~500 Ma, indicative that this sample may contain Palaeozoic zircon populations.

Sm-Nd geochemistry

The ε_{Nd} results are shown in the Sm-Nd whole-rock data table in the supplementary material and are plotted on Figures 8 and 9 to demonstrate the geochemical variations with spatial reference to the MCT zone. The data range in $\varepsilon_{Nd(0)}$ from -27.7 to -12.1.

Discussion

The magmatic history

The Palaeoproterozoic granites ('Lingtse gneiss') from the MCT zone were originally dated using Rb-Sr, yielding ages of c.1075-2034 Ma (Paul et al. 1982; Paul et al. 1996). The Lingtse gneiss samples from the Sikkim Himalaya analysed in this study provide an age cluster within error between 1834 ± 37 Ma and 1853 ± 19 Ma (Fig. 4) and may be age-correlated with other Lesser Himalayan granite gneisses across the Himalaya (Goswami et al. 2009; see Table 1 from Kohn et al. 2010 for summary of ages). This widespread Palaeoproterozoic magmatic event has been ascribed to a continental volcanic arc that was active during the formation of the supercontinent Columbia (Kohn et al. 2010).

Samples 32, 115 and 280 analysed in this study yield ages of 829 ± 28 Ma, 604 ± 28 Ma and 508 ± 22 Ma (Fig. 5). These orthogneiss ages are consistent with similar meta-igneous intrusion ages from the GHS elsewhere in the Himalaya. These include an event at ~500 Ma (Bhargava 1995; Marquer et al. 2000; Miller et al. 2001; Ghosh et al. 2005; Richards et al. 2005) and an earlier Neoproterozoic event at ~800 Ma (DiPietro and Isachsen 2001; Singh et al. 2002; Ghosh et al. 2005; Richards et al. 2006; Spencer et al. 2012). A widespread Cambro-Ordovician tectonic event has been documented across the GHS (Argles et al. 1999; Marquer et al. 2000; Gehrels et al. 2003; Gehrels et al. 2006). This has been termed the 'Bhimphedian orogeny' (Cawood et al. 2007), and has been related to the Cambrian formation of Gondwana (Yin et al. 2010b).

The significance of the ~800 Ma magmatism is somewhat more enigmatic but has been tentatively linked to the presence of a superplume beneath the Rodinian continent resulting in intracontinental rifting (Li et al. 2008). This has been linked to the Malani magmatic event (750 Ma) on the Indian craton, during which volcanism resulted from the final rifting and break-up of this part of the supercontinent (Sharma 2005). The precise cause of the magmatism at this time remains unclear, but suggestions include back-arc extension (Zhou et al. 2002), the arrival of a mantle plume (Guynn et al. 2012), or post-orogenic slab break off (Wang et al. 2006).

The MCT zone in the Sikkim Himalaya

The geochronological and geochemical data from this study can be categorised into two isotopic groups, shown in Fig. 8. The samples with detrital zircon ages that show a dominant peak at ~1800 Ma, with no zircons younger than ~1700 Ma (Fig. 6), and those samples with an εNd signature of -27.7 to -23.4, are indicative of an LHS signature when compared to the published literature as reviewed above. The youngest detrital zircons in the LHS sediments are coeval to the granite intrusion ages, which date from ~1800 Ma. The samples that have a detrital zircon age signature which ranges down to younger than 800 Ma (Fig. 7) or an εNd signature of -18.3 to -12.1 can be characterised as GHS samples when compared to previous studies. The youngest concordant Greater Himalayan detrital zircons are roughly contemporaneous with the oldest granite intrusion (~800 Ma), suggesting that these were deposited in an active tectonic environment.

It has recently been suggested that the significance of detrital age information is obscured in some Himalayan regions, because some of the Lesser Himalayan formations overlap in characteristics with some of the Greater Himalayan lithologies (Myrow et al. 2010). The LHS units in the eastern Himalaya are divided into three quite distinct supracrustal formations (Fig. 1): the Palaeoproterozoic Daling formation, the Neoproterozoic-Cambrian Buxa formation and the much younger Permian Gondwana sediments. Whereas the Buxa and Gondwana sediments (sometimes termed the Outer Lesser Himalaya, Richards et al. 2005) have an isotopic signature that can overlap with the GHS (McQuarrie et al. 2013), the older predominant Daling unit has an isotopic signature which contrasts markedly with that of the GHS, producing a geochemical contrast across the thrust zone wherever the Daling and GHS are juxtaposed, such as in the Sikkim Himalaya.

The geochemical and geochronological characterisation of the samples from this study has allowed for a more precise trace of the MCT to be proposed in the Sikkim Himalaya (Fig. 2b), which is generally consistent with that presented in Rubatto et al. (2012). Our study, which presents the first isotopic data from the rocks of the Sikkim Himalaya, demonstrates that rocks sometimes mapped as

296 a separate lithological unit, the 'MCT zone' (Fig. 2a), are primarily of Daling Lesser Himalayan
297 isotopic affinity. This is an important conclusion because it implies that the deformation associated
298 with the MCT has mainly penetrated downwards from the "protolith boundary" marked by a distinct
299 break in isotopic signature and granite intrusion age, several kilometres into the footwall of the
300 structure. The deformation associated with thrust faults is known to migrate down into the footwall
301 of the structure when there is progressive failure of the footwall ramps. This results in the
302 abandonment of the old thrust surface and the development of new thrusts in the footwall that
303 eventually leads to the formation of an imbricate stack (Butler 1982). This suggests that as
304 movement on the MCT occurred in the Sikkim Himalaya at ~22-10 Ma (Catlos et al. 2004),
305 deformation migrated down-section from the original isotopic break, interpreted as the location of
306 the original décollement zone of the MCT, into the underlying Lesser Himalayan rocks.

307 ***Tectonic imbrication***

308 Three transects (Figs 9a, b and c) provide exceptions to the simple division between the hanging wall
309 and footwall of the MCT, as outlined above. Samples in these locations yield abrupt out-of-
310 sequence, alternating shifts in ε_{Nd} and detrital zircon characteristics in a ~5-10 km thick zone (shown
311 as outliers in Figure 8). This has important implications both for the geochemical "fingerprinting" of
312 rock units on either side of the MCT, and potentially other obscure ductile faults with major
313 displacements worldwide, and for understanding the mechanics of thrusting.

314 There are several possible alternative explanations for these shifts:

315 **i) Fluid alteration**

316 The Sm–Nd system could have been perturbed by fluid alteration or some other process, giving an
317 anomalous signature. However, the unperturbed Sm/Nd values (~0.11) for the rocks measured in
318 this study do not support significant disturbance of the Sm–Nd system (Ahmad et al. 2000).

319 **ii) Sediment sources**

It has been proposed that the Paro and Jaishidanda sequences in Bhutan were deposited in a tectonically active, distal foreland basin associated with the 'Bhimpedian' orogeny, affected by shifts in sediment source with material sourced from both the GHS rocks (younger detritus) and the Indian shield (older detritus) (McQuarrie et al. 2013). The Bhutan sequences probably correlate to the along-strike MCT zone of the Sikkim Himalaya. Sample 292 in this study lacks a prominent 1800 Ma detrital zircon peak and has a larger spread of older zircons than other typical 'LHS' rocks (Fig. 6), potentially supporting the theory of different sediment sources for certain rocks within the MCT zone.

The 'interleaved' signatures could therefore reflect abrupt shifts in the nature of detritus being deposited in the MCT zone sedimentary protoliths (Tobgay et al. 2011; McQuarrie et al. 2013). These shifts could result from one or more of the following: 1) specific depositional settings, 2) sediment transport processes, and 3) erosion processes in the catchments.

A marine depositional environment is indicated for MCT zone rocks in the Sikkim Himalaya by the abundance of tourmaline (implying high boron concentrations; Carrano et al. 2009), and the interbedding of pelites and quartzites. In the relatively near-shore (delta or continental shelf) setting suggested by these lithologies, sediment can be deposited in a dynamic environment (Allen 2005), which could explain the observed abrupt shifts in geochemical signature in different rock packages. However, the dispersal of sediment from rivers into marine systems may be unpredictable (Wright and Nittrouer 1995), suggesting that detritus from a single river can become dispersed and mixed with other sediment, causing signatures of individual rivers to be obscured in the final depositional marine setting. The abrupt shifts in geochemical signature we observed in the Sikkim Himalaya would require very distinct sediment sources for certain rocks, with little basin-scale mixing.

Differences in isotopic signature between two sedimentary packages may also be due to a difference in their duration of transport, and hence time of deposition. For instance, it has been proposed that

grain size can act as a buffer, with larger grains (i.e. in the quartzite) being transported faster to the final deposition site than the finer grains that characterise the pelitic lithologies (Allen 2007).

The third controlling factor could have been changes in the catchment and erosion areas of rivers in a tectonically active region. Recent work has shown that the route of the Yarlung-Tsangpo-Irrawaddy system was modified by river capture during Himalayan uplift (Robinson et al. 2013). A similar catchment shift could have occurred during the Palaeozoic, perhaps associated with uplift during the Bhimpedian orogeny when the GHS rocks were deposited. However, such shifts in river catchment are likely to result in a single switching of sediment source and isotopic signature; since we observe repeated reversals of the signatures, this scenario seems less likely in the Sikkim Himalaya.

In a marine sedimentary environment any shifts in erosion, deposition or river catchment would be recorded as progressive, not abrupt, changes in the sedimentary record. In addition, the alternating geochemical signatures of packages in the Sikkim Himalaya are uniquely associated with proximity to the MCT (Fig. 8). Moreover our observation, based on detailed geochemical studies, that rock packages characterised by specific detrital isotopic signatures are intruded by granite intrusions of contrasting ages favours a tectonic explanation. Overall, we do not consider that the evidence provided in this study supports a purely sedimentological interpretation of the variation of isotopic signatures.

iii) Tectonic interleaving

The observed signature of the rocks could have been caused by tectonic interleaving of LHS and GHS rocks associated with the tectonic movement along the MCT. This model is supported by evidence in Figures 9a and 9b where narrow slivers of pelites are exposed that yield distinct ε_{Nd} signatures from their immediately adjacent orthogneisses and pelites with contrasting geochemical signature. Since such complexities are only found in the area surrounding the MCT, we suggest that ductile shearing was involved in determining the observed spatial distribution of the hanging wall and footwall rocks.

368 This study is not the first to discover tectonic complications associated with the MCT. Gansser (1991)
369 observed that the MCT can form either a “zone of imbrication or can expose a sharp contact”. Our
370 work confirms that there may be along-strike geochemical and structural variations and complexities
371 regarding the nature of the MCT. To the east, detrital zircon and ε_{Nd} signatures from the Paro
372 window in Bhutan (Tobgay et al. 2011) are also suggestive of an imbricate zone similar to the MCT in
373 the Sikkim Himalaya. This has important implications for the tectonic affinity of the Paro
374 metasedimentary rocks, and may suggest that the Yadong cross-structure (Fig. 1; Cooper et al. 2012
375 and references therein) does not mark a fundamental orogenic break separating contrasting
376 protolith sources for the constituent metasedimentary lithologies. There are also examples of mixing
377 around the MCT to the west. Although Martin et al. (2005) found no evidence of an imbricate zone
378 associated with the MCT in the Annapurna region of western Nepal, Parrish and Hodges (1996)
379 termed a relatively narrow conspicuous zone of lithological and structural imbrication around the
380 MCT in the Langtang region of central Nepal as the “MCT imbricate zone”, characterised by $\varepsilon_{Nd(0)}$
381 signatures of -16.3 to -21.4. This latter study suggested that variations in the ε_{Nd} ratios in this zone
382 showed that the MCT zone was formed from interleaving of slices of both footwall and hanging wall
383 rocks. Studies in other Nepal transects have also reported ambiguous overlapping ε_{Nd} signatures
384 from the vicinity of the MCT, which could also be interpreted as evidence for imbrication (Robinson
385 et al. 2001; Imayama and Arita 2008).

386 Although major brittle thrust faults can form a single sharp contact (Butler 1982; Law 1998),
387 imbrication and duplexing is more likely to develop in a ductile thrust system. The development of
388 new thrusts in the footwall of structures may lead to piggyback thrusting and the development of a
389 duplex (Butler 1982) and has been identified in the LHS rocks of the Sikkim Himalaya (Bhattacharyya
390 and Mitra 2009). A similar process could occur in ductile structures, with subsequent reworking
391 making it difficult to identify. A mixing zone can be seen in thrust faults around the world on a
392 variety of scales, from centimetres thick (Dickinson 1991), to a few minor structures over the
393 lengthscale of metres (Gilotti and Kumpulainen 1986; Yonkee 1997), to large-scale structures over

hundreds to metres (Barr 1986; Holdsworth and Strachan 1991; Gilotti and McClelland 2008; Leslie et al. 2010). A similar setting to the MCT we describe in the Sikkim Himalaya is identified in the Caledonian orogenic belt in eastern Greenland, where imbricate slices, tens of metres thick, are interleaved by ductile thrusting in a zone of inverted metamorphism (Holdsworth and Strachan 1991). In the case of the Sikkim Himalaya, structural evidence for imbrication may be difficult to recognise in a zone of progressive ductile deformation due to subsequent reworking. Geochemical 'fingerprinting' therefore provides a complementary and potentially more robust tool for identifying such imbrication within any major ductile shear zone.

Provenance and tectonic implications

Several regional studies have proposed that the Lesser Himalayan/Greater Himalayan/Tethyan sediments were deposited on the proximal (LHS) to distal (GHS) parts of the passive margin of India (Brookfield 1993; Myrow et al. 2003; Myrow et al. 2010). Cenozoic movement on the MCT juxtaposed these once widely separated parts of the Indian continent. We have developed a model for the provenance and pre-Himalayan architecture of the eastern Himalaya, constrained by the geochemical data presented in this study (Fig. 10).

The model shows that Lesser Himalayan Daling and subsequent Buxa sediments were deposited on the proximal margin of India. The Daling sediments were intruded by granites, probably in a continental arc-type setting, during the Palaeoproterozoic (Kohn et al. 2010). Palaeoproterozoic zircons from the granites were transported out to the more distal parts of the margin where the Greater Himalayan rocks were deposited. The Neoproterozoic magmatism (820-850 Ma) may relate to a plume-related intracratonic rift separating the LHS and GHS sedimentary basins of the margin (Li et al. 2008). This would explain the exposure of the distal GHS sediments to the Cambro-Ordovician Bhimphedian orogeny, in marked contrast to the more southerly, proximal, LHS package that was apparently unaffected by this event (Fig. 10).

418 The juxtaposition of the exposed parts of the GHS and LHS postdates the 500 Ma event. During the
419 early stages of the India-Asia collision, following the subduction of the Tethys Ocean, the Mesozoic
420 and Palaeozoic succession on the northern flank of the Indian continental margin was thickened and
421 deformed, causing tectonic burial and prograde metamorphism of the underlying GHS package.
422 Following this burial and northward subduction of the Neoproterozoic-Mesozoic northern Indian
423 margin, the GHS sediments were detached from their (unknown) depositional basement along a
424 deep-seated décollement (the proto-MCT) and began to be translated southwards, while undergoing
425 syn-metamorphic deformation. It is possible that the MCT exploited the closed, failed
426 Neoproterozoic rift as the thrust propagated southwards, which could help to explain the striking
427 coincidence of the MCT with the isotopic break along the entire Himalaya. Progressive convergence
428 and crustal thickening triggered extrusion of the ductile and weak GHS between the South Tibetan
429 Detachment and the Main Central thrust, which transported the GHS 140-500 kilometres over the
430 previously proximal Lesser Himalayan rocks that originally lay to the south (Dewey et al. 1989;
431 Schelling and Arita 1991; Brookfield 1993; Robinson et al. 2006; Tobgay et al. 2012; Webb 2013). The
432 ductile deformation and associated inverted metamorphism in the footwall of the MCT suggest that
433 some Daling sediments were both strongly deformed and heated during MCT motion, as heat was
434 transferred from the hotter GHS rocks above. Simultaneous footwall heating and hanging wall
435 cooling caused the inverted metamorphism which straddles the hanging wall-footwall contact. The
436 Sikkim Himalaya can therefore be seen as preserving a mid-crustal section of the ductile shear zone
437 associated with the MCT. In this ductile setting, ramps and flats on the MCT resulted in imbrication
438 or interleaving of the LHS and GHS in the immediate vicinity of the thrust. Deformation was
439 subsequently transferred to the Ramgarh thrust (Pearson and DeCelles 2005; Webb 2013; Robinson
440 and Pearson 2013), which was responsible for finally exhuming the deformed Daling rocks in its
441 hanging wall and thrusting them upon the Buxa rocks, inverting the original Daling-Buxa sedimentary
442 relationship in the LHS (Fig. 2c).

Conclusions

The Sikkim Himalaya exposes a window into a well-preserved mid-crustal thrust zone formed during the Himalayan orogeny. New geochemical and geochronological data show that there is a significant isotopic break between the juxtaposed LHS and GHS packages in this region. The GHS rocks are characterised by detrital zircon age peaks at ~800-1000 Ma, 1500-1700 Ma and 2300-2500 Ma and by an $\varepsilon Nd_{(0)}$ signature of -18.3 to -12.1. This rock package was intruded by granites of Neoproterozoic (~800 Ma) and Ediacaran-Cambrian (~500-600 Ma) age. In contrast, the Daling part of the LHS rocks comprise a Palaeoproterozoic rock package with prominent Archaean and Palaeoproterozoic detrital zircon populations and an $\varepsilon Nd_{(0)}$ signature of -27.7 to -23.4. These rocks were intruded by Palaeoproterozoic granites but not by the younger granites seen in the hanging wall. The Lesser and Greater Himalayan sediments represent older/more proximal, and younger/more distal parts of the Indian margin respectively. The two packages have been juxtaposed over several hundred kilometres by Cenozoic thrusting along the mid-crustal shear zone exposed at the surface in the Sikkim Himalaya. The deformation associated with the MCT has penetrated down into the Lesser Himalayan rocks of the footwall forming a zone of progressive ductile shearing.

In detail, the data show significant apparent out-of-sequence isotopic signatures in some locations, consistent with local imbrication. These isotopic anomalies are interpreted as representing slices of footwall and hanging wall that became locally interleaved during protracted deformation. Similar isotopic anomalies have previously been reported along strike eastwards, in the 'Paro Window' of Bhutan. This similarity suggests that these rocks may be of similar protolith and have experienced similar tectonic disruption, placing constraints on the amount of displacement caused by the intervening, Yadong cross structure.

Isotope geochemistry is a robust tool for defining differences between and the juxtaposition of two distinct terranes across a structure which spans over 2500 kilometres along the Himalayan orogen.

It is equally useful for resolving tectonic problems that have proved intractable to conventional structural methods. This approach is applicable to studies of other orogenic interiors where detailed footwall-hanging wall relationships of major terrane boundaries have been obscured by pervasive ductile shearing.

Acknowledgments

This study was funded by a UK Natural Environmental Research Council PhD studentship awarded to Catherine Mottram. We thank Sam Hammond for technical support with TIMS and ICP-MS analyses. Thanks to Vanessa Pashley and Nick Roberts for technical support with LA-MC-ICP-MS and AttoM work at NIGL and to Adrian Wood and Tony Miladowski, for other technical support at NIGL/BGS. Thanks in particular to Kesang Sherpa and Tenpa Ji for excellent driving in Sikkim and Lucy Greenwood and Souvik Mitra for help with Indian logistics and assistance in the field. Thanks to reviews from Aaron Martin, Kip Hodges and editor comments from Bernard Bingen that significantly improved the manuscript. Finally, thanks to Mike Searle who critically reviewed an earlier draft of this paper and provided useful suggestions for improvement.

References

Acharyya, S. 1975. Structure and stratigraphy of the Darjeeling frontal zone, Eastern Himalaya. *Miscellaneous publications of the Geological Survey of India,* **24,** 71-90.

Ahmad, T., Harris, N., Bickle, M., Chapman, H., Bunbury, J. & Prince, C. 2000. Isotopic constraints on the structural relationships between the Lesser Himalayan Series and the High Himalayan Crystalline Series, Garhwal Himalaya. *Geological Society of America Bulletin,* **112,** 467-477.

Allen, P. 2005. Striking a chord. *Nature* **434,** 961-961

Allen, P. A. 2008. Time scales of tectonic landscapes and their sediment routing systems. *Geological Society, London, Special Publications* **296** 7-28.

Ameen, S. M. M., Wilde, S. A., Kabir, Z., Akon, E., Chowdhury, K. R. & Khan, S. H. 2007. Paleoproterozoic granitoids in the basement of Bangladesh: A piece of the Indian shield or an exotic fragment of the Gondwana jigsaw? *Gondwana Research,* **12,** 380-387.

Argles, T., Prince, C., Foster, G. & Vance, D. 1999. New garnets for old? Cautionary tales from young mountain belts. *Earth and Planetary Science Letters,* **172,** 301-309.

496 Banerjee, H., Dasgupta, S., Bhattacharyya, P. K. & Sarkar, S. C. 1983. Evolution of the Lesser
497 Himalayan Metapelites of the Sikkim- Darjeeling region, India, and some related problems.
498 *Neues Jahrbuch für Mineralogie - Abhandlungen,* **146**.

499 Barr, D., Holdsworth, R.E. & Roberts, A.M. 1986. Caledonian ductile thrusting in a Precambrian
500 metamorphic complex: The Moine of northwestern Scotland. *Geological Society of America*
501 *Bulletin* **97** 754-764.

502 Bhargava, O. N. 1995. The Bhutan Himalaya: A geological Account. *Geological Survey of India Special*
503 *Publication,* **39**.

504 Bhattacharyya, K. & Mitra, G. 2009. A new kinematic evolutionary model for the growth of a duplex -
505 an example from the Rangit duplex, Sikkim Himalaya, India. *Gondwana Research,* **16,** 697-
506 715.

507 Bhattacharyya, K. & Mitra, G. 2011. Strain softening along the MCT zone from the Sikkim Himalaya:
508 Relative roles of Quartz and Micas. *Journal of Structural Geology,* **33,** 1105-1121.

509 Bordet, P. 1961. *Recherches géologiques dans l'Himalaya du Nepal, région du Makalu: Expéditions*
510 *françaises à l'Himalaya 1954-1955, organisées par la Fédération de la montagne en*
511 *coopération avec leClub alpin français. Mission scientifique du CNRS*, Ed. du Centre national
512 de la recherche scientifique.

513 Butler, R. W. 1982. The terminology of structures in thrust belts. *Journal of Structural Geology* **4** 239-
514 245.

515 Brookfield, M. E. 1993. The Himalayan passive margin from PreCambrian to Cretaceous times.
516 *Sedimentary Geology,* **84,** 1-35.

517 Carrano, C.J., Schellenberg, S. Amin, S.A., Green, D.H. & Küpper, F.C. 2009. Boron and Marine Life: A
518 New Look at an Enigmatic Bioelement. *Marine Biotechnology,* **11**, 431-440.

519 Catlos, E. J., Dubey, C. S., Harrison, T. M. & Edwards, M. A. 2004. Late Miocene movement within the
520 Himalayan Main Central Thrust shear zone, Sikkim, north-east India. *Journal of Metamorphic*
521 *Geology,* **22,** 207-226.

522 Catlos, E. J., Harrison, T. M., Kohn, M. J., Grove, M., Ryerson, F. J., Manning, C. E. & Upreti, B. N.
523 2001. Geochronologic and thermobarometric constraints on the evolution of the Main
524 Central Thrust, central Nepal Himalaya. *Journal of Geophysical Research-Solid Earth,* **106,**
525 16177-16204.

526 Cawood, P. A., Johnson, M.R. & Nemchin, A.A. 2007. Early Palaeozoic orogenesis along the
527 Indian margin of Gondwana: Tectonic response to Gondwana assembly. *Earth and*
528 *Planetary Science Letters* **255** 70-84.

529 Chakraborty, S., Dasgupta, S. & Neogi, S. 2003. Generation of migmatites and the nature of partial
530 melting in a continental collision zone setting: an example from the Sikkim Himalaya. *Indian*
531 *journal of geology,* **75,** 38-53.

532 Cooper, F., Adams, B., Edwards, C. & Hodges, K. 2012. Large normal-sense displacement on the
533 South Tibetan fault system in the eastern Himalaya. *Geology,* **40,** 971-974.

534 Daniel, C. G., Hollister, L. S., Parrish, R. R. & Grujic, D. 2003. Exhumation of the Main Central Thrust
535 from lower crustal depths, Eastern Bhutan Himalaya. *Journal of Metamorphic Geology,* **21,**
536 317-334.

537 Dasgupta, S., Ganguly, J. & Neogi, S. 2004. Inverted metamorphic sequence in the Sikkim Himalayas:
538 crystallization history, P-T gradient and implications. *Journal of Metamorphic Geology,* **22,**
539 395-412.

540 Dasgupta, S., Chakraborty, S. & Neogi, S. 2009. Petrology of an inverted Barrovian Sequence of
541 metapelites in Sikkim Himalaya, India: Constraints on the tectonics of inversion. *American*
542 *Journal of Science,* **309**, 43-84.

543 Davidson, C., Crujic, D., Hollister, L. & Schmid, S. 1997. Metamorphic reactions related to
544 decompression and synkinematic intrusion of leucogranite, High Himalayan Crystallines,
545 Bhutan. *Journal of Metamorphic Geology,* **15,** 593-612.

546 Dewey, J., Cande, S. & Pitman, W. C. 1989. Tectonic evolution of the India/Eurasia collision zone.
547 *Eclogae Geologicae Helvetiae,* **82,** 717-734.

548 Dickinson, W. R. 1991. *Tectonic Setting of Faulted Tertiary Strata Associated With the Catalina Core*
549 *Complex in Southern Arizona*, *Book and Geological Map*, GSA Bookstore.

550 DiPietro, J. A. & Isachsen, C. E. 2001. U-Pb zircon ages from the Indian plate in northwest Pakistan
551 and their significance to Himalayan and pre-Himalayan geologic history. *Tectonics,* **20,** 510-
552 525.

553 Dubey, C. S., Catlos, E. J. & Sharma, B. K. 2005. Modelling of P-T-t paths constrained by mineral
554 chemistry and monazite dating of metapelites in relationship to MCT activity in Sikkim
555 Eastern Himalayas. *In:* Thomas, H. (ed.) *In: Metamorphism and Crustal Evolution.* New Delhi:
556 Atlantic publishers.

557 Gansser, A. 1983. *Geology of the Bhutan Himalaya*, Birkhčauser Verlag, Basel.

558 Gansser, A. 1991. Facts and theories on the Himalayas. *Eclogae Geologicae Helvetiae,* **84,** 33-59.

559 Gehrels, G., DeCelles, P., Martin, A., Ojha, T., Pinhassi, G. & Upreti, B. 2003. Initiation of the
560 Himalayan orogen as an early Paleozoic thin-skinned thrust belt. *GSA TODAY,* **13,** 4-9.

561 Gehrels, G., DeCelles, P., Ojha, T. & Upreti, B. 2006. Geologic and U-Th-Pb geochronologic evidence
562 for early Paleozoic tectonism in the Kathmandu thrust sheet, central Nepal Himalaya.
563 *Geological Society of America Bulletin,* **118,** 185-198.

564 Gehrels, G., Kapp, P., DeCelles, P., et al. 2011. Detrital zircon geochronology of pre-Tertiary strata in
565 the Tibetan-Himalayan orogen. *Tectonics,* **30**.

566 Ghosh, A. M. N. 1956. Recent advances in geology and structure of Eastern Himalaya. *Proceedings of*
567 *the Indian Science Congress,* **44,** 85-99.

568 Ghosh, S., Fallick, A. E., Paul, D. K. & Potts, P. J. 2005. Geochemistry and origin of Neoproterozoic
569 granitoids of Meghalaya, Northeast India: Implications for linkage with amalgamation of
570 Gondwana Supercontinent. *Gondwana Research,* **8,** 421-432.

571 Gilotti, J. A. & Kumpulainen, R. 1986. Strain softening induced ductile flow in the Särv thrust sheet,
572 Scandinavian Caledonides. *Journal of Structural Geology* **8** 441-455.

573 Gilotti, J. A. & McClelland, W. C. 2008. Geometry, kinematics and timing of extensional faulting in the
574 Greenland Caledonides–a synthesis. *Memoirs of the Geological Society of America* **202** 251-
575 271.

576 Goswami, S. 2005. *Inverted metamorphism in the Sikkim-Darjeeling Himalaya: Structural,*
577 *metamorphic and numerical studies.* Doctor of Philosophy, University of Cambridge.

578 Goswami, S., Bhowmik, S. K. & Dasgupta, S. 2009. Petrology of a non-classical Barrovian inverted
579 metamorphic sequence from the western Arunachal Himalaya, India. *Journal of Asian Earth*
580 *Sciences,* **36,** 390-406.

581 Greenwood, L. V. 2013. *Orogenesis in the Eastern Himalayas: A study of structure, geochronology*
582 *and metamorphism in Bhutan.* PhD, The Open University.

583 Groppo, C., Rolfo, F. & Lombardo, B. 2009. P-T Evolution across the Main Central Thrust Zone
584 (Eastern Nepal): Hidden Discontinuities Revealed by Petrology. *Journal of Petrology,* **50,**
585 1149-1180.

586 Gupta, S., Das, A., Goswami, S., Modak, A. & Mondal, S. 2010. Evidence for Structural Discordance in
587 the Inverted Metamorphic Sequence of Sikkim Himalaya: Towards Resolving the Main
588 Central Thrust Controversy. *Journal of the Geological Society of India,* **75,** 313-322.

589 Guynn, J., Kapp, P., Gehrels, G. E. & Ding, L. 2012. U–Pb geochronology of basement rocks in central
590 Tibet and paleogeographic implications. *Journal of Asian Earth Sciences,* **43,** 23-50.

591 Hamilton, P. J., O'Nions, R. K., Bridgwater, D. & Nutman, A. 1983. Sm-Nd studies of Archaean
592 metasediments and metavolcanics from West Greenland and their implications for the
593 Earth's early history. *Earth and Planetary Science Letters,* **62,** 263-272.

Harrison, T. M., Ryerson, F. J., LeFort, P., Yin, A., Lovera, O. M. & Catlos, E. J. 1997. A Late Miocene-Pliocene origin for the Central Himalayan inverted metamorphism. *Earth and Planetary Science Letters,* **146,** E1-E7.

Heim, A. A. & Gansser, A. 1939. *Central Himalaya: Geological observations of the Swiss expedition, 1936*, Hindustan Publication Corporation, India.

Holdsworth, R. E. & Strachan, R.A. 1991. Interlinked system of ductile strike slip and thrusting formed by Caledonian sinistral transpression in northeastern Greenland. *Geology* **19,** 510-513.

Hubbard, M. S. & Harrison, T. M. 1989. 40Ar/39Ar age constraints on deformation and metamorphism in the Main Central Thrust zone and Tibetan Slab, eastern Nepal Himalaya. *Tectonics,* **8,** 865-880.

Imayama, T. & Arita, K. 2008. Nd isotopic data reveal the material and tectonic nature of the Main Central Thrust zone in Nepal Himalaya. *Tectonophysics,* **451,** 265-281.

Inger, S. & Harris, N. 1993. Geochemical constraints on leucogranite magmatism in the Langtang Valley, Nepal Himalaya. *Journal of Petrology,* **34,** 345-368.

Kohn, M. J., Catlos, E. J., Ryerson, F. J. & Harrison, T. M. 2001. Pressure-temperature-time path discontinuity in the Main Central thrust zone, central Nepal. *Geology,* **29,** 571-574.

Kohn, M. J., Paul, S. K. & Corrie, S. L. 2010. The lower Lesser Himalayan sequence: A Paleoproterozoic arc on the northern margin of the Indian plate. *Geological Society of America Bulletin,* **122,** 323-335.

Law, R. 1998. Quartz mylonites from the Moine thrust zone at the Stack of Glencoul, Northwest Scotland. *Fault-Related Rocks: A Photographic Atlas*. Princeton University Press, Princeton, New Jersey. 490-493.

Le Fort, P. 1975. Himalayas: The collided range. Present knowledge of the continental arc. *American Journal of Science,* **275,** 1 - 44.

Leslie, A., Krabbendam, M., Kimbell, G.S. & Strachan, R.A. 2010. Regional-scale lateral variation and linkage in ductile thrust architecture: the Oykel Transverse Zone, and mullions, in the Moine Nappe, NW Scotland. *Geological Society, London, Special Publications* **335**, 359-381.

Li, Z., Bogdanova, S., Collins, A. S., et al. 2008. Assembly, configuration, and break-up history of Rodinia: a synthesis. *Precambrian Research,* **160,** 179-210.

Long, S., McQuarrie, N., Tobgay, T. & Grujic, D. 2011a. Geometry and crustal shortening of the Himalayan fold-thrust belt, eastern and central Bhutan. *Geological Society of America Bulletin,* **123,** 1427-U1244.

627 Long, S., McQuarrie, N., Tobgay, T., Rose, C., Gehrels, G. & Grujic, D. 2011b. Tectonostratigraphy of
628 the Lesser Himalaya of Bhutan: Implications for the along-strike stratigraphic continuity of
629 the northern Indian margin. *Geological Society of America Bulletin,* **123,** 1406-1426.

630 Macfarlane, A. M., Hodges, K. V. & Lux, D. 1992. A structural analysis of the Main Central Thrust
631 zone, Langtang National Park, Central Nepal Himalaya. *Geological Society of America*
632 *Bulletin,* **104,** 1389-1402.

633 Marquer, D., Chawla, H. S. & Challandes, N. 2000. Pre-alpine high-grade metamorphism in High
634 Himalaya crystalline sequences: Evidence from Lower palaeozoic Kinnaur Kailas granite and
635 surrounding rocks in the Sutlej Valley (Himachal Pradesch, India). *Eclogae Geologicae*
636 *Helvetiae,* **93,** 207-220.

637 Martin, A. J., Burgy, K.D., Kaufman, A.J. & Gehrels, G.E.2011. Stratigraphic and tectonic implications
638 of field and isotopic constraints on depositional ages of Proterozoic Lesser Himalayan rocks
639 in central Nepal. *Precambrian Research***, 185**, 1-17.

640 Martin, A. J., DeCelles, P. G., Gehrels, G. E., Patchett, P. J. & Isachsen, C. 2005. Isotopic and structural
641 constraints on the location of the Main Central thrust in the Annapurna Range, central Nepal
642 Himalaya. *Geological Society of America Bulletin,* **117,** 926-944.

643 Martin, A., Ganguly, J. & DeCelles, P. 2010. Metamorphism of Greater and Lesser Himalayan rocks
644 exposed in the Modi Khola valley, central Nepal. *Contributions to Mineralogy and Petrology,*
645 **159,** 203-223.

646 McLennan, S., McCulloch, M., Taylor, S. & Maynard, J. 1989. Effects of sedimentary sorting on
647 neodymium isotopes in deep-sea turbidites. *Nature,* **337,** 547-549.

648 McQuarrie, N., Long, S. P., Tobgay, T., Nesbit, J. N., Gehrels, G. & Ducea, M. N. 2013. Documenting
649 basin scale, geometry and provenance through detrital geochemical data: Lessons from the
650 Neoproterozoic to Ordovician Lesser, Greater, and Tethyan Himalayan strata of Bhutan.
651 *Gondwana Research,* **23,** 1491-1510.

652 McQuarrie, N., Robinson, D., Long, S., Tobgay, T., Grujic, D., Gehrels, G. & Ducea, M. 2008.
653 Preliminary stratigraphic and structural architecture of Bhutan: Implications for the along
654 strike architecture of the Himalayan system. *Earth and Planetary Science Letters,* **272,** 105-
655 117.

656 Miller, C., Thoni, M., Frank, W., Grasemann, B., Klotzli, U., Guntli, P. & Draganits, E. 2001. The early
657 Palaeozoic magmatic event in the Northwest Himalaya, India: source, tectonic setting and
658 age of emplacement. *Geological Magazine,* **138,** 237-251.

659 Myrow, P. M., Hughes, N. C., Goodge, J. W., et al. 2010. Extraordinary transport and mixing of
660 sediment across Himalayan central Gondwana during the Cambrian–Ordovician. *Geological*
661 *Society of America Bulletin,* **122,** 1660-1670.

662 Myrow, P. M., Hughes, N. C., Paulsen, T. S., et al. 2003. Integrated tectonostratigraphic analysis of
663 the Himalaya and implications tor its tectonic reconstruction. *Earth and Planetary Science*
664 *Letters,* **212,** 433-441.

665 Neogi, S., Dasgupta, S. & Fukuoka, M. 1998. High P-T polymetamorphism, dehydration melting, and
666 generation of migmatites and granites in the Higher Himalayan Crystalline Complex, Sikkim,
667 India. *Journal of Petrology,* **39,** 61-99.

668 Parrish, R. R. & Hodges, K. V. 1996. Isotopic constraints on the age and provenance of the Lesser and
669 Greater Himalayan sequences, Nepalese Himalaya. *Geological Society of America Bulletin,*
670 **108,** 904-911.

671 Passchier, C. W. & Trouw, R. A. J. 2005. *Microtectonics*, Springer.

672 Paul, D. K., Chandy, K. C., Bhalla, J. K., Prasad, R. & Sengupta, P. 1982. Geochronology and
673 geochemistry of the Lingtse Gneiss, Darjeeling-Sikkim Himalaya. *Indian journal of Earth*
674 *Sciences,* **9,** 11-17.

675 Paul, D. K., McNaughton, N. J., Chattopadhyay, S. & Ray, K. K. 1996. Geochronology and
676 geochemistry of the Lingtse gneiss, Darjeeling-Sikkim Himalaya: Revisited. *Journal of the*
677 *Geological Society of India,* **48,** 497-506.

678 Pearson, O. N. & DeCelles, P. G. 2005. Structural geology and regional tectonic significance of the
679 Ramgarh thrust, Himalayan fold-thrust belt of Nepal. *Tectonics,* **24,** TC4008.

680 Pêcher, A. 1989. The metamorphism in the central Himalaya. *Journal of Metamorphic Geology,* **7,** 31-
681 41.

682 Pin, C. & Zalduegui, J. S. 1997. Sequential separation of light rare-earth elements, thorium and
683 uranium by miniaturized extraction chromatography: Application to isotopic analyses of
684 silicate rocks. *Analytica Chimica Acta,* **339,** 79-89.

685 Richards, A., Argles, T., Harris, N., Parrish, R., Ahmad, T., Darbyshire, F. & Draganits, E. 2005.
686 Himalayan architecture constrained by isotopic tracers from clastic sediments. *Earth and*
687 *Planetary Science Letters,* **236,** 773-796.

688 Richards, A., Parrish, R., Harris, N., Argles, T. & Zhang, L. 2006. Correlation of lithotectonic units
689 across the eastern Himalaya, Bhutan. *Geology,* **34,** 341-344.

690 Robinson, D. M., DeCelles, P. G., Patchett, P. J. & Garzione, C. N. 2001. The kinematic evolution of
691 the Nepalese Himalaya interpreted from Nd isotopes. *Earth and Planetary Science Letters,*
692 **192,** 507-521.

693 Robinson, D. M., DeCelles, P.G. & Copeland,P. 2006. Tectonic evolution of the Himalayan thrust belt
694 in western Nepal: Implications for channel flow models. *Geological Society of America*
695 *Bulletin***, 118**, 865-885.

696 Robinson, D. M. & Pearson, O.N. 2013. Was Himalayan normal faulting triggered by initiation of the
697 Ramgarh–Munsiari thrust and development of the Lesser Himalayan duplex? *International*
698 *Journal of Earth Sciences* 1-18.

699 Robinson, R. A., Brezina, C.A., Parrish, R.R., et al. 2013. Large rivers and orogens: The evolution of the
700 Yarlung Tsangpo-Irrawaddy system and the eastern Himalayan syntaxis. *Gondwana*
701 *Research. In press*

702 Rubatto, D., Chakraborty, S. & Dasgupta, S. 2013. Timescales of crustal melting in the Higher
703 Himalayan Crystallines (Sikkim, Eastern Himalaya) inferred from trace element-constrained
704 monazite and zircon chronology. *Contributions to Mineralogy and Petrology* **165**, 349-372.

705 Schelling, D. & Arita, K. 1991. Thrust tectonics, crustal shortening, and the structure of the far-
706 eastern Nepal Himalaya *Tectonics,* **10,** 851-862.

707 Searle, M. P., Law, R. D., Godin, L., Larson, K. P., Streule, M. J., Cottle, J. M. & Jessup, M. J. 2008.
708 Defining the Himalayan Main Central Thrust in Nepal. *Journal of the Geological Society,* **165,**
709 523-534.

710 Searle, M. P. & Szulc, A. G. 2005. Channel flow and ductile extrusion of the high Himalayan slab - the
711 Kangchenjunga-Darjeeling profile, Sikkim Himalaya. *Journal of Asian Earth Sciences,* **25,** 173-
712 185.

713 Sharma, K. K. 2005. Malani magmatism: An extensional lithospheric tectonic origin. *Special Papers*
714 *Geological Society of America,* **388,** 463.

715 Singh, S., Barley, M. E., Brown, S. J., Jain, A. K. & Manickavasagam, R. M. 2002. SHRIMP U-Pb in zircon
716 geochronology of the Chor granitoid: evidence for Neoproterozoic magmatism in the Lesser
717 Himalayan granite belt of NW India. *Precambrian Research,* **118,** 285-292.

718 Spencer, C. J., Harris, R. A. & Dorais, M. J. 2012. Depositional provenance of the Himalayan
719 metamorphic core of Garhwal region, India: Constrained by U-Pb and Hf isotopes in zircons.
720 *Gondwana Research,* **22,** 26-35.

721 Stäubli, A. 1989. Polyphase metamorphism and the development of the Main Central Thrust. *Journal*
722 *of Metamorphic Geology,* **7,** 73-93.

723 Stephenson, B. J., Searle, M. P., Waters, D. J. & Rex, D. C. 2001. Structure of the Main Central Thrust
724 zone and extrusion of the High Himalayan deep crustal wedge, KishtwarÂ–Zanskar Himalaya.
725 *Journal of the Geological Society,* **158,** 637-652.

726 Thomas, R., Jacobs, J., Horstwood, M., Ueda, K., Bingen, B. & Matola, R. 2010. The Mecubúri and Alto
727 Benfica groups, NE Mozambique: aids to unravelling ca. 1 and 0.5 Ga events in the east
728 African orogen. *Precambrian Research,* **178,** 72-90.

729 Thomas, R. J., Roberts, N. M. W., Jacobs, J., Bushi, A. M., Horstwood, M. S. A. & Mruma, A. 2013.
730 Structural and geochronological constraints on the evolution of the eastern margin of the

731 Tanzania Craton in the Mpwapwa area, central Tanzania. *Precambrian Research,* **224,** 671-
732 689.

733 Tobgay, T., Long, S., McQuarrie, N., Ducea, M. N. & Gehrels, G. 2011. Using isotopic and chronologic
734 data to fingerprint strata: Challenges and benefits of variable sources to tectonic
735 interpretations, the Paro Formation, Bhutan Himalaya. *Tectonics,* **29**.

736 Tobgay, T., McQuarrie, N., Long, S., Kohn, M. J. & Corrie, S. L. 2012. The age and rate of displacement
737 along the Main Central Thrust in the western Bhutan Himalaya. *Earth and Planetary Science*
738 *Letters,* **319-320,** 146-158.

739 Valdiya, K. S. 1980. *Geology of Kumaun Lesser Himalaya*, Wadia Institute of Himalayan Geology
740 Dehradun.

741 Vermeesch, P. 2004. How many grains are needed for a provenance study? *Earth and Planetary*
742 *Science Letters,* **224,** 441-451.

743 Wang, X.-L., Zhou, J.-C., Qiu, J.-S., Zhang, W.-L., Liu, X.-M. & Zhang, G.-L. 2006. LA-ICP-MS U-Pb zircon
744 geochronology of the Neoproterozoic igneous rocks from Northern Guangxi, South China:
745 Implications for tectonic evolution. *Precambrian Research,* **145,** 111-130.

746 Webb, A. A. G. 2013. Preliminary balanced palinspastic reconstruction of Cenozoic deformation
747 across the Himachal Himalaya (northwestern India). *Geosphere ,* **9**, 572-587.

748 Webb, A. A. G., Yin, A. & Dubey, C. S. 2013. U-Pb zircon geochronology of major lithologic units in the
749 eastern Himalaya: Implications for the origin and assembly of Himalayan rocks. *Geological*
750 *Society of America Bulletin,* **125,** 499-522.

751 Whittington, A., Foster, G., Harris, N., Vance, D. & Ayres, M. 1999. Lithostratigraphic correlations in
752 the western Himalaya - An isotopic approach. *Geology,* **27,** 585-588.

753 Wright, L. & Nittrouer, C. 1995. Dispersal of river sediments in coastal seas: six contrasting cases.
754 *Estuaries* **18**, 494-508.

755 Yin, A., Dubey, C. S., Kelty, T. K., Webb, A. A. G., Harrison, T. M., Chou, C. Y. & Celerier, J. 2010a.
756 Geologic correlation of the Himalayan orogen and Indian craton: Part 2. Structural geology,
757 geochronology, and tectonic evolution of the Eastern Himalaya. *Geological Society of*
758 *America Bulletin,* **122,** 360-395.

759 Yin, A., Dubey, C. S., Webb, A. A. G., Kelty, T. K., Grove, M., Gehrels, G. E. & Burgess, W. P. 2010b.
760 Geologic correlation of the Himalayan orogen and Indian craton: Part 1. Structural geology,
761 U-Pb zircon geochronology, and tectonic evolution of the Shillong Plateau and its
762 neighboring regions in NE India. *Geological Society of America Bulletin,* **122,** 336-359.

763 Yonkee, W. 1997. Part 4: Kinematics and Mechanics of theWillard Thrust Sheet, Central Part of the
764 Sevier Orogenic Wedge, North-central Utah. *Brigham Young University Geology Studies.* **42,**
765 341-354.

766 Zhou, M.-F., Yan, D.-P., Kennedy, A. K., Li, Y. & Ding, J. 2002. SHRIMP U–Pb zircon geochronological
767 and geochemical evidence for Neoproterozoic arc-magmatism along the western margin of
768 the Yangtze Block, South China. *Earth and Planetary Science Letters,* **196,** 51-67.

769 **Figure Captions**

770 **Fig. 1.** Geological sketch map of the central and eastern Himalayas. Adapted from McQuarrie et al.
771 2008 and Greenwood, 2013.

772 **Fig. 2. a**) Geological map of Sikkim based on previous maps of the area [Goswami, 2005; Gupta et al.
773 2010]. Insets for Figures 3 and 9. **b**) Geological map of Sikkim modified from data presented in this
774 study with key sample locations (further sample locations are shown in Figure 9). Line of section
775 presented for Figure 2c. **c**) Sketch geological cross section, with no vertical exaggeration (line of
776 section shown in Figure 2b) from data presented in this study. Lesser Himalayan Duplex taken from
777 Bhattacharyya and Mitra, 2009. Abbreviations are the same as in Figure 1.

778 **Fig. 3.** Summary of structural features beneath the MCT in Mangan transect, North Sikkim. A)
779 Stretched quartz vein boudinage. B) L-tectonite fabric in Lingtse orthogneiss. C) Shear bands in
780 garnet-mica schists. D) Stretching lineation developed in an orthogneiss intruding chlorite-grade
781 metasedimentary rocks (note colour changes are weathering on fractured surfaces rather than veins
782 of melt). The orthogneiss body displays a more developed stretching lineation than the surrounding
783 rocks indicating how contrasting lithologies accommodate strain differently. Localities of the
784 photographs are shown on map, top right of figure. Map units as for Figures 1 and 2.

785 **Fig. 4.** Orthogneiss concordia plots (1). Ages for each sample are reported as average $^{207}Pb/^{206}Pb$
786 ages with 2SD uncertainties. The MSWD of the population is quoted and reflects excess scatter in
787 the Pb/Pb data. Sample locations shown in inset map.

788 **Fig. 5.** Orthogneiss concordia plots (2). Ages for each sample are reported as average $^{207}Pb/^{206}Pb$
789 ages with 2SD uncertainties. The MSWD of the population is quoted and reflects excess scatter in
790 the Pb/Pb data. Sample locations shown in inset map.

Fig. 6. Data for detrital zircon in clastic metasedimentary samples (1): concordia plots reporting all analyses; probability density plots based on analyses with discordance lower than 5%. Sample locations shown in inset map.

Fig. 7. Data for detrital zircon in clastic metasedimentary samples (2): concordia plots reporting all analyses; probability density plots based on analyses with discordance lower than 5%. Sample locations shown in inset map.

Fig. 8. Plot of a) εNd signature and b) detrital zircon and orthogneiss U-Pb age, as a function of depth above and below the MCT (positive numbers=up section into GHS and negative numbers= down section into LHS). The MCT is defined here as the protolith boundary as outlined in the text and in Fig. 2b. The LHS/GHS classification is based on previous Himalayan studies; these signatures overlap slightly in the zircon plot (b) marked by the hatched area. The LHS signature however does not extend younger than 1700 Ma. There are three outliers marked with arrows which demonstrate the location of proposed interleaved slices.

Fig. 9. Detailed maps of combined Nd and U-Pb isotopic data. **a**) Kalimpong-Lava transect. **b**) Pelling-Dentam-Yoksom transect. **c**) Mangan transect. Geological units are the same as in legend in Figures 1-2. 'Imbricate zone', as discussed in the text, is shown in grey. Large numbers preceded by minus signs are εNd values; εNd values for GHS surrounded by black box. Small numbers in italics are sample locations. Orthogneiss ages are shown in circles (dashed line for LHS values and solid line for GHS samples). Detrital zircons populations are shown as probability density plots or as a rectangular dashed outline box (Fig. 9a). Full concordia and probability density plots can be found in Figures 4-7.

Fig. 10. Schematic cartoon showing the pre-Himalayan architecture of the Sikkim rocks, during the mid-Palaeozoic. The LHS lithologies were once separated from the GHS rocks by a Neoproterozoic rift. The Bhimpedian orogeny was responsible for closing the rift and thickened the GHS, causing

814 metamorphism and intrusion of granites. The failed closed rift may represent a weak structure later

815 exploited by the MCT. Lithologies are the same as in legend in Figures 1-2.

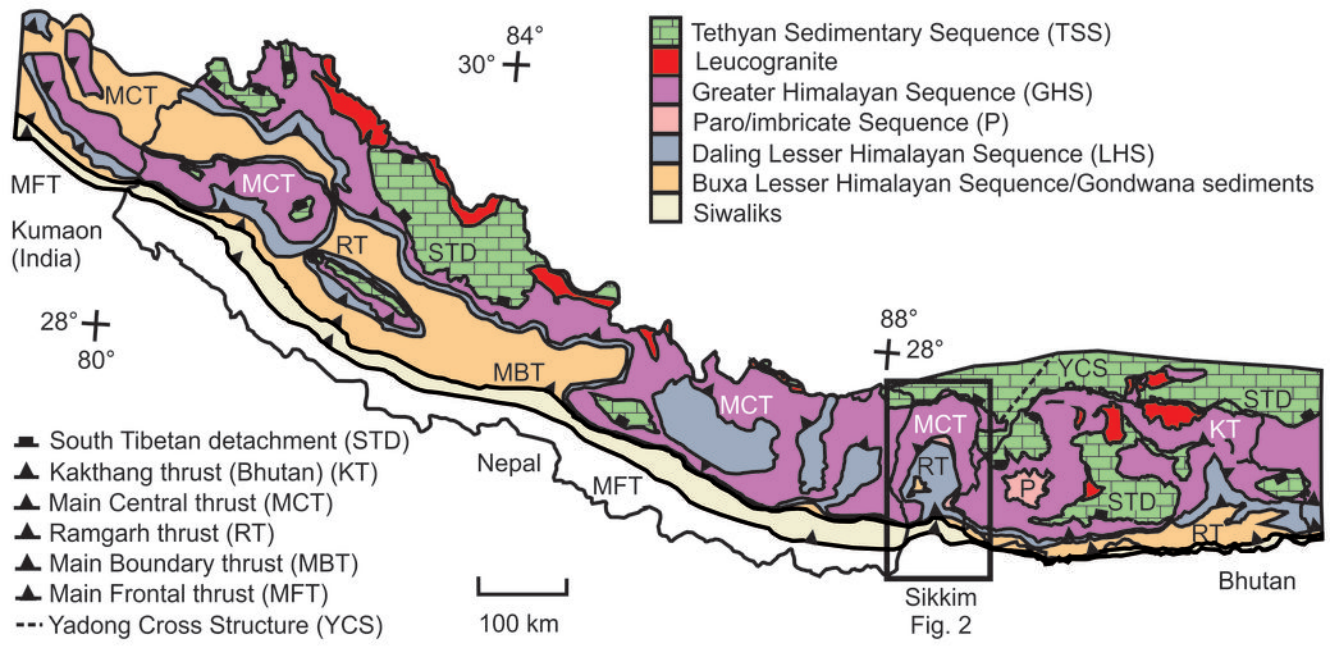
Tethyan Sedimentary Sequence (TSS)
Leucogranite
Greater Himalayan Sequence (GHS)
Paro/imbricate Sequence (P)
Daling Lesser Himalayan Sequence (LHS)
Buxa Lesser Himalayan Sequence/Gondwana sediments
Siwaliks
84°
30°
MCT
MFT
Kumaon
(India)
MCT
RT
STD
28°
80°
MBT
MCT
88°
28°
YCS
STD
MCT
KT
RT
P
STD
RT
Bhutan
South Tibetan detachment (STD)
Kakthang thrust (Bhutan) (KT)
Main Central thrust (MCT)
Ramgarh thrust (RT)
Main Boundary thrust (MBT)
Main Frontal thrust (MFT)
Yadong Cross Structure (YCS)
Nepal
MFT
100 km
Sikkim
Fig. 2

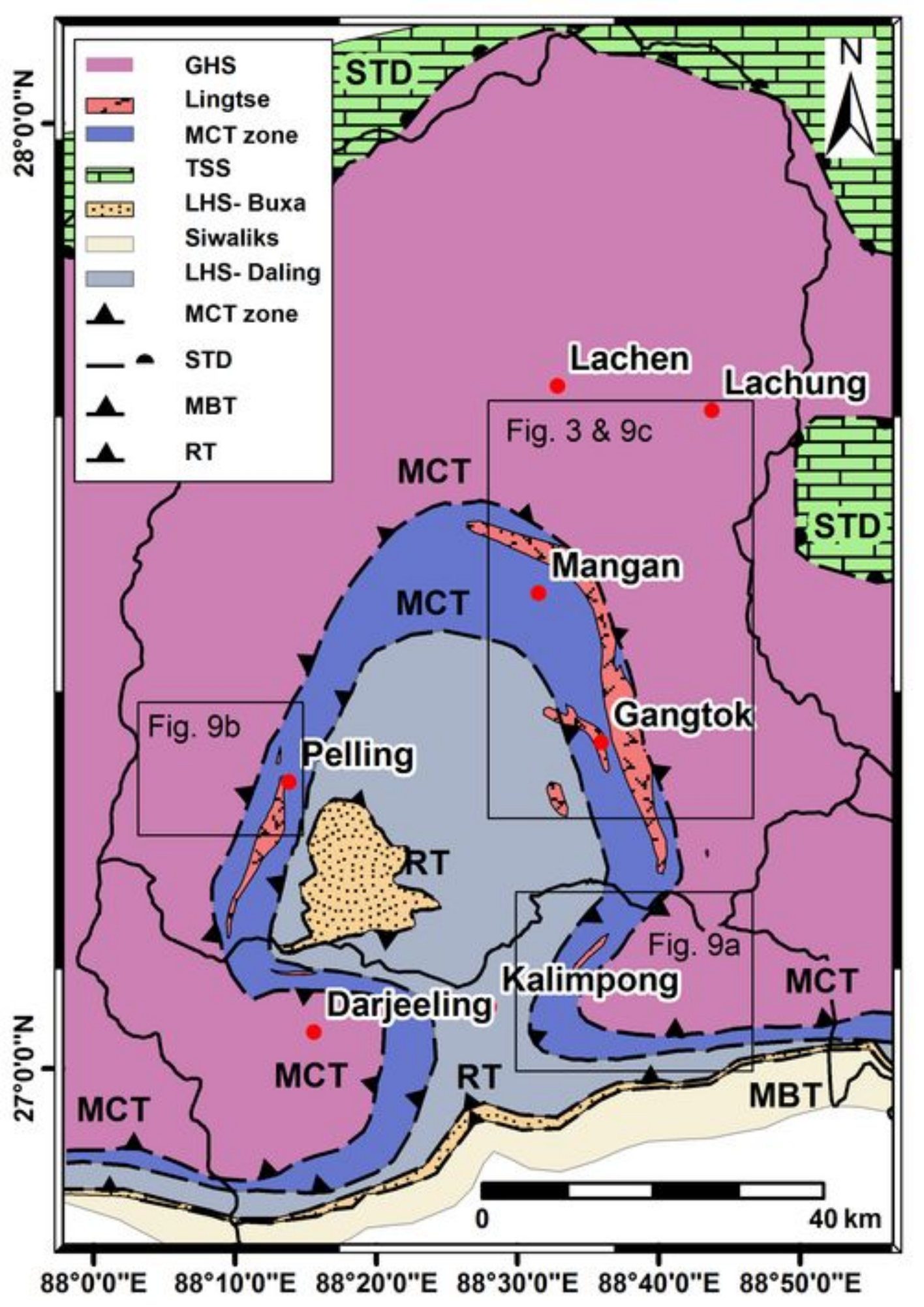
GHS
Lingtse
MCT zone
TSS
LHS- Buxa
Siwaliks
LHS- Daling
MCT zone
STD
MBT
RT
N
STD
Lachen
Lachung
Fig. 3 & 9c
MCT
STD
Mangan
MCT
Gangtok
Fig. 9b
Pelling
RT
Fig. 9a
Kalimpong
MCT
Darjeeling
MCT
RT
MBT
MCT
0
40 km
28°0'0"N
27°0'0"N
88°0'0"E
88°10'0"E
88°20'0"E
88°30'0"E
88°40'0"E
88°50'0"E

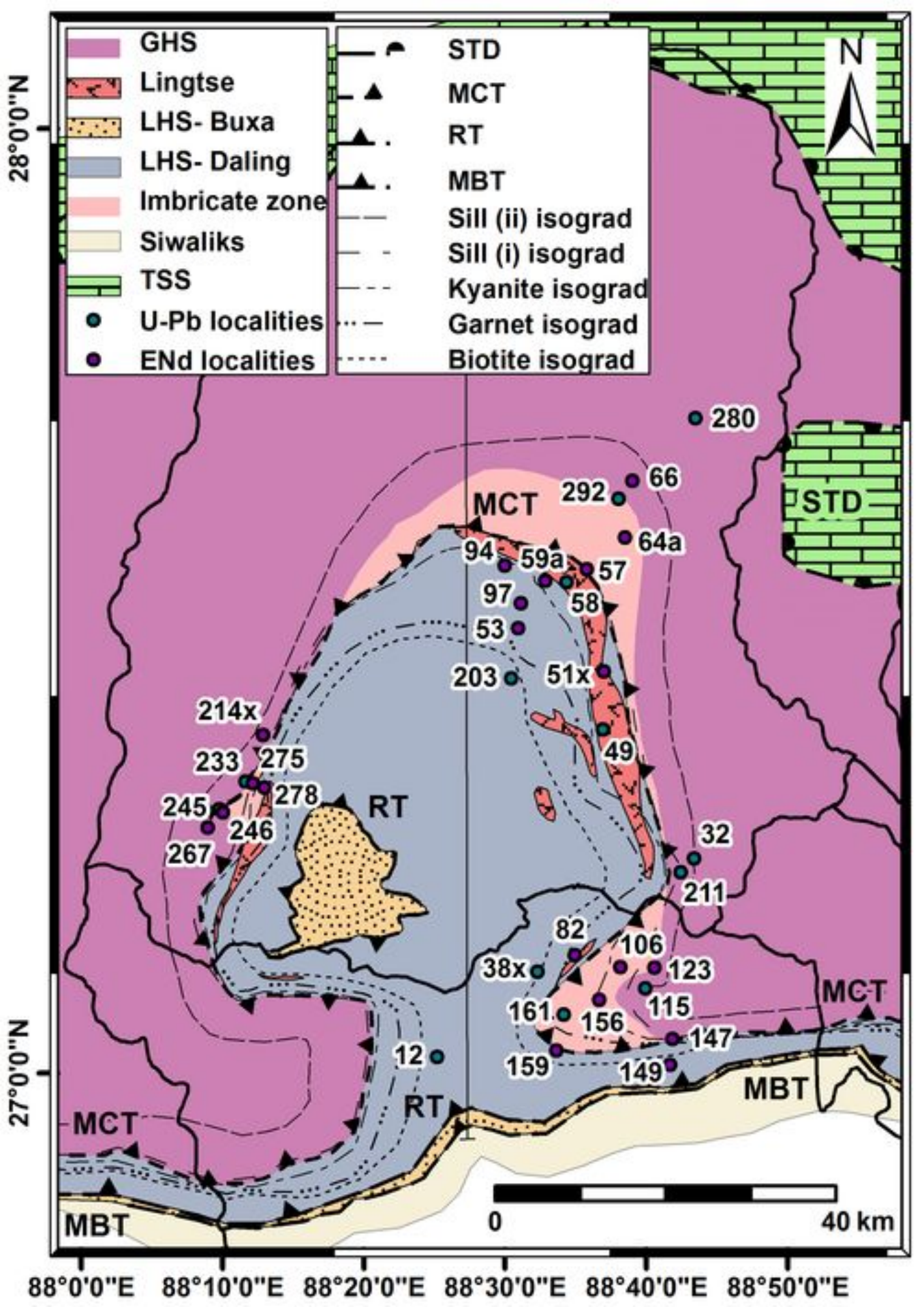
GHS
Lingtse
LHS- Buxa
LHS- Daling
Imbricate zone
Siwaliks
TSS
U-Pb localities
ENd localities
STD
MCT
RT
MBT
Sill (ii) isograd
Sill (i) isograd
Kyanite isograd
Garnet isograd
Biotite isograd
N
280
66
292
64a
94
59a
57
97
58
53
203
51x
49
214x
233
275
278
245
246
267
32
211
82
106
38x
123
115
161
156
147
159
149
12
0
40 km
28°0'0"N
27°0'0"N
88°0'0"E
88°10'0"E
88°20'0"E
88°30'0"E
88°40'0"E
88°50'0"E

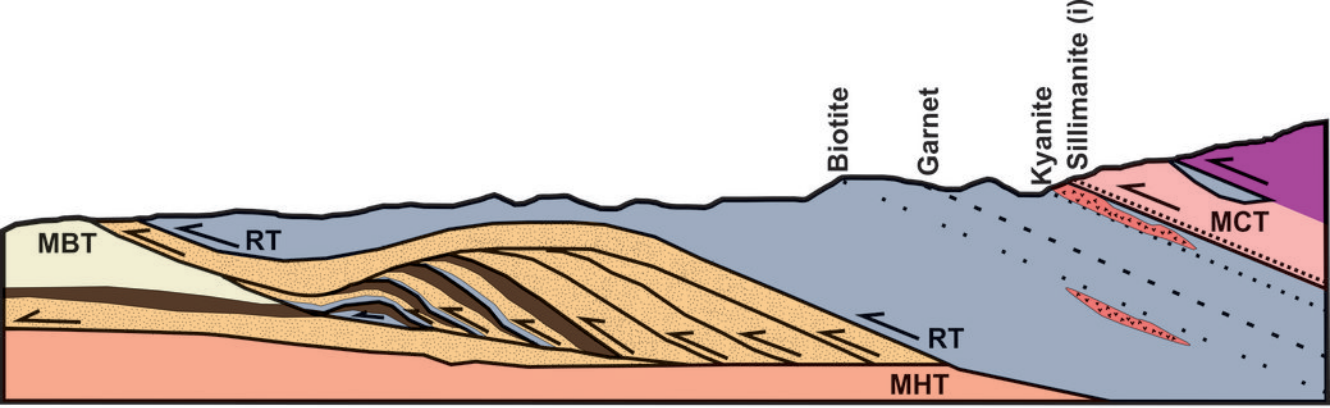

20 Km

Main Central thrust (MCT)
Ramgarh thrust (RT)
Main Boundary thrust (MBT)
Main Himalayan thrust (MHT)

Greater Himalayan Sequence (GHS)
Imbricate zone
Lesser Himalayan Sequence Daling (LHS)
Lingtse Orthogneiss
Lesser Himalayan Sequence Buxa (LHS)
Gondwana sediments
Siwaliks

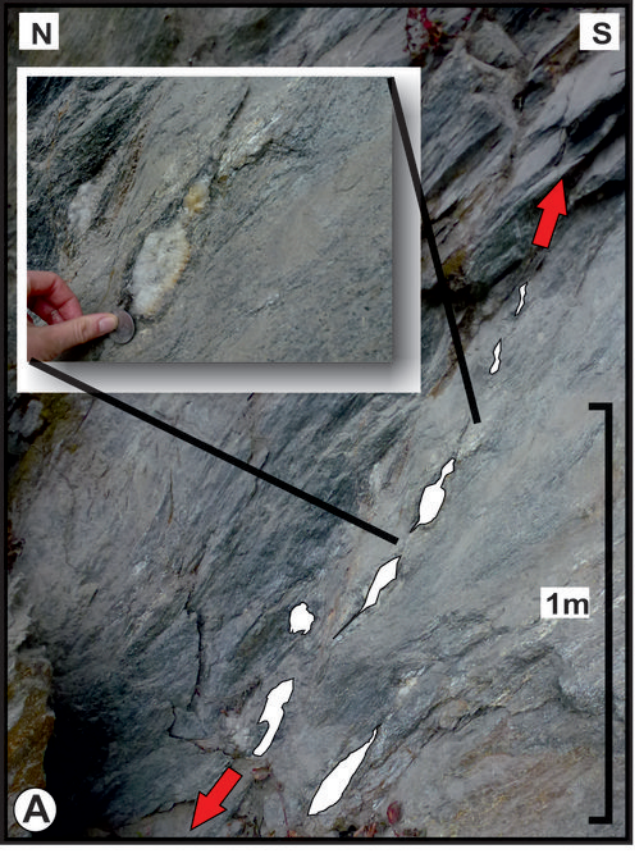
N
S
1m
A

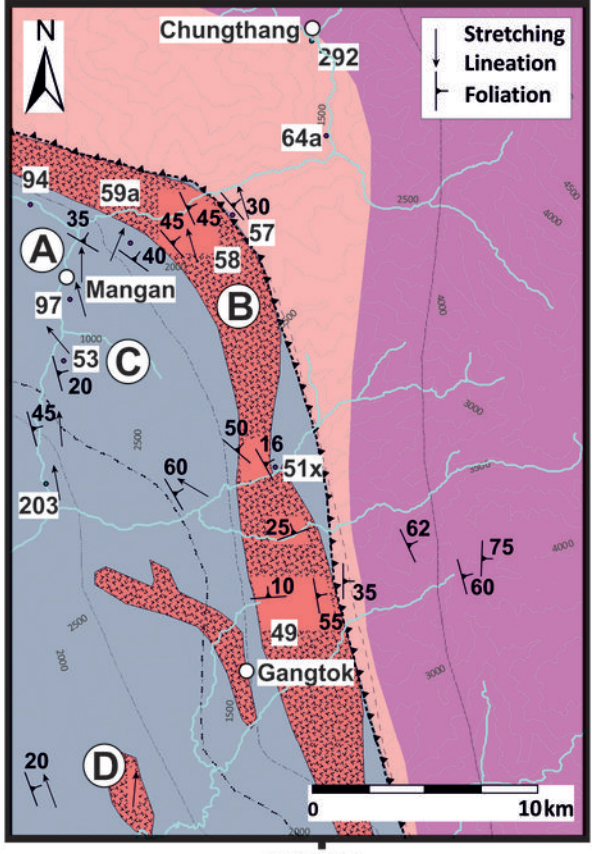
N
Chungthang
292
Stretching Lineation
Foliation
64a
94
59a
30
57
45
45
35
40
58
A
Mangan
97
B
53
20
C
45
50
16
51x
60
203
25
62
75
60
10
35
55
49
Gangtok
20
D
0
10km
88°40'E


E
W
1m

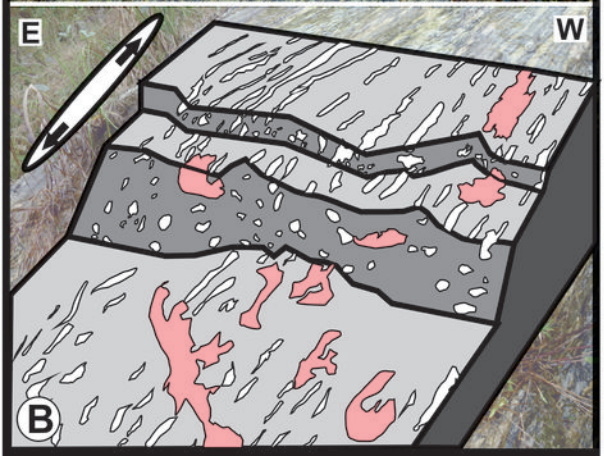
E
W
B

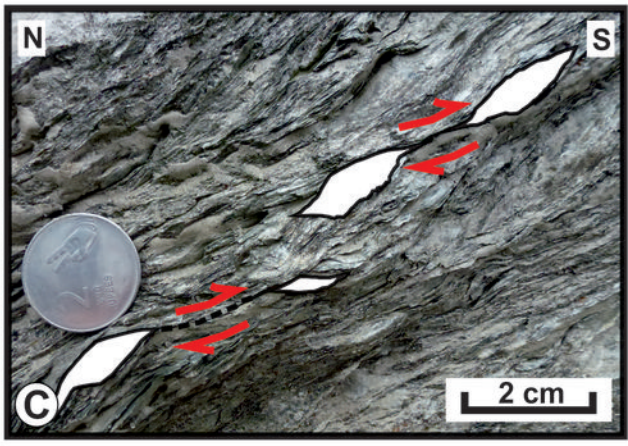
N
S
C
2 cm

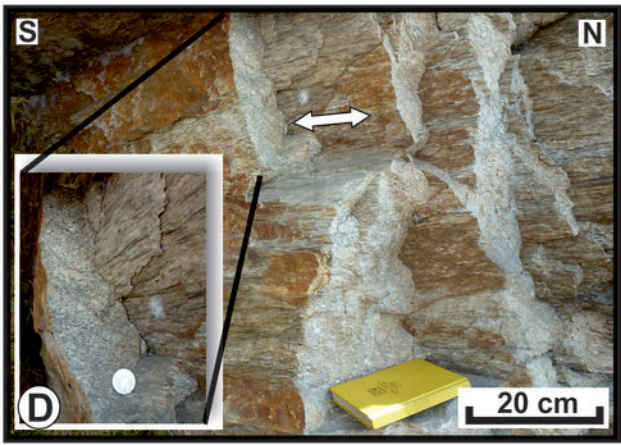
S
N
D
20 cm

Orthogneiss samples

Sample 49
1837 ± 45 Ma (2σ)
MSWD 11.6 (n= 13)

Sample 58
1836 ± 26 Ma (2σ)
MSWD 11.5 (n=14)

Sample 233
1834 ± 37 Ma (2σ)
MSWD 20 (n=18)

Sample 245
1853 ± 19 Ma (2σ)
MSWD 17
(n=25)

1 analysis
>2400 Ma

2400
2200
2000
1800
1600

$^{206}Pb/^{238}U$

$^{207}Pb/^{235}U$

data-point error
ellipses are 2σ

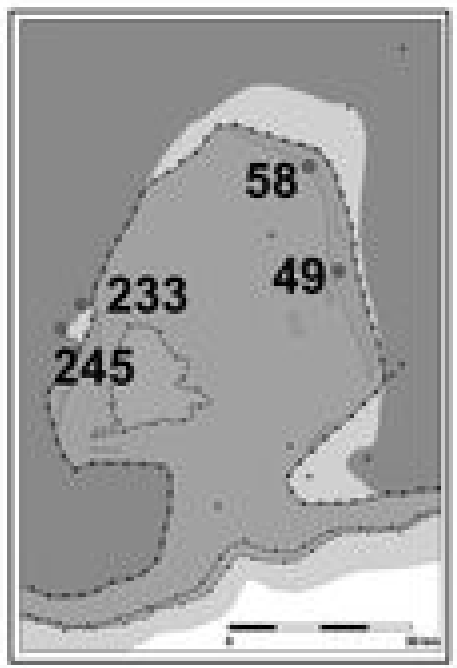

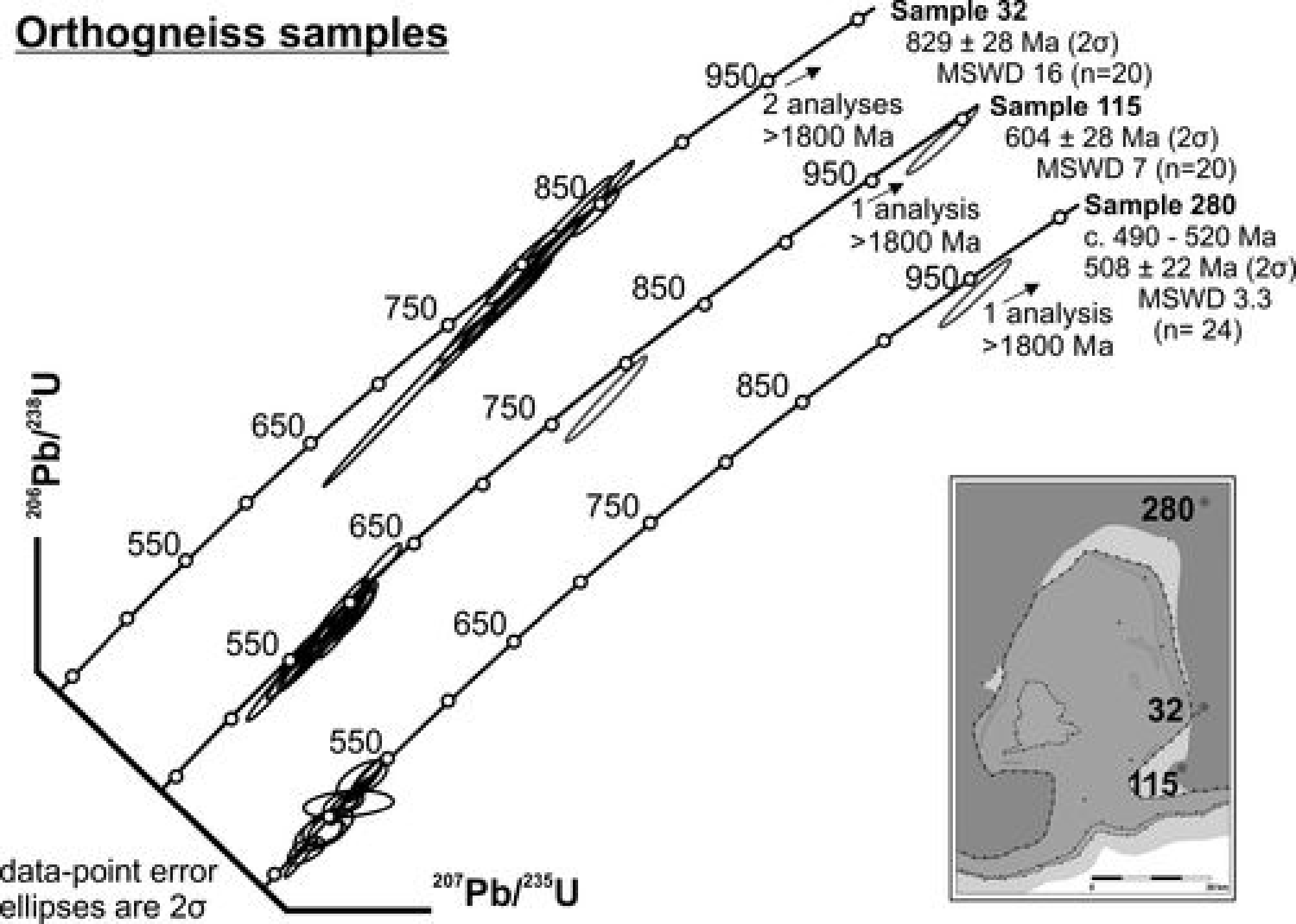
Orthogneiss samples
Sample 32
829 ± 28 Ma (2σ)
MSWD 16 (n=20)
2 analyses
>1800 Ma
Sample 115
604 ± 28 Ma (2σ)
MSWD 7 (n=20)
1 analysis
>1800 Ma
Sample 280
c. 490 - 520 Ma
508 ± 22 Ma (2σ)
MSWD 3.3
(n= 24)
1 analysis
>1800 Ma
950
850
750
650
550
206Pb/238U
207Pb/235U
data-point error
ellipses are 2σ
280
32
115

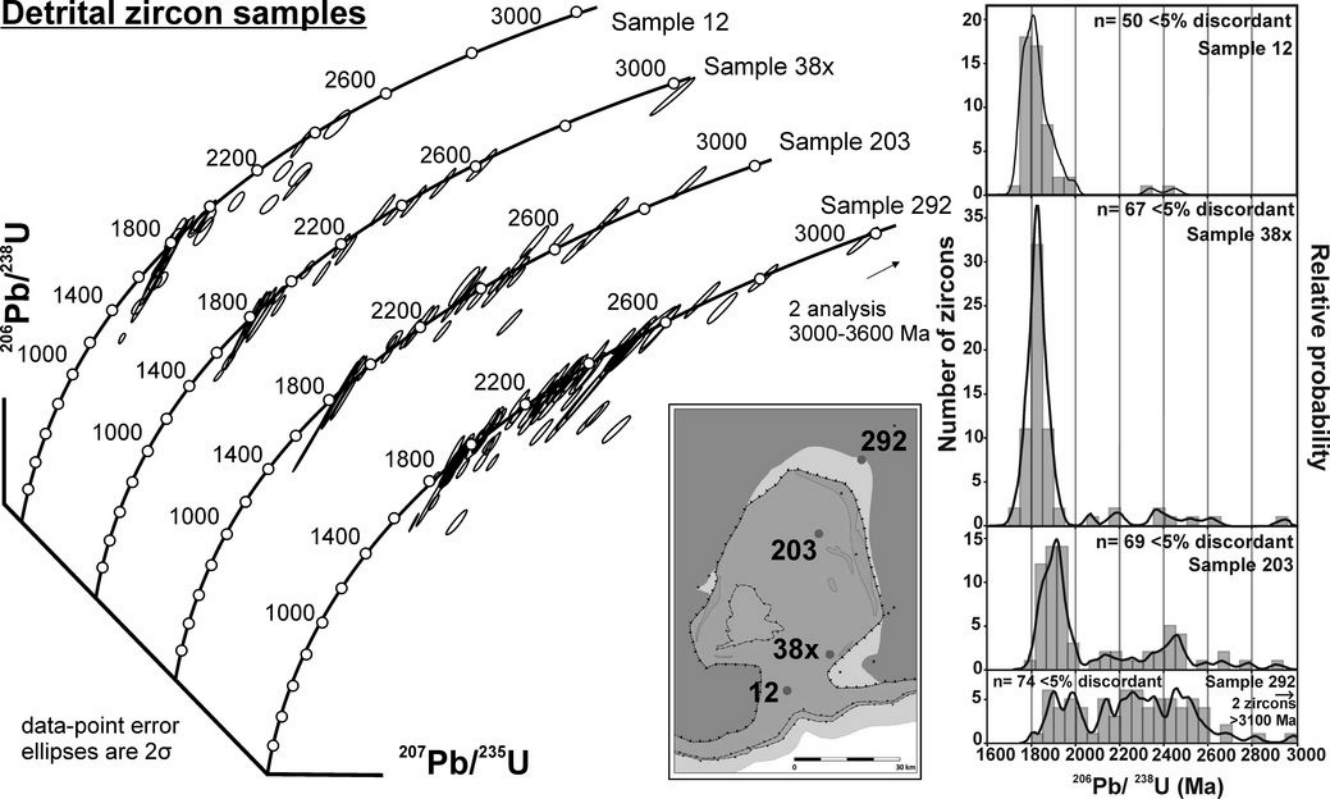
Detrital zircon samples
Sample 12
Sample 38x
Sample 203
Sample 292
2 analysis
3000-3600 Ma
$^{206}Pb/^{238}U$
$^{207}Pb/^{235}U$
data-point error
ellipses are 2σ
292
203
38x
12
0
30 km
n= 50 <5% discordant
Sample 12
n= 67 <5% discordant
Sample 38x
n= 69 <5% discordant
Sample 203
n= 74 <5% discordant
Sample 292
2 zircons
>3100 Ma
Number of zircons
Relative probability
$^{206}Pb/^{238}U$ (Ma)

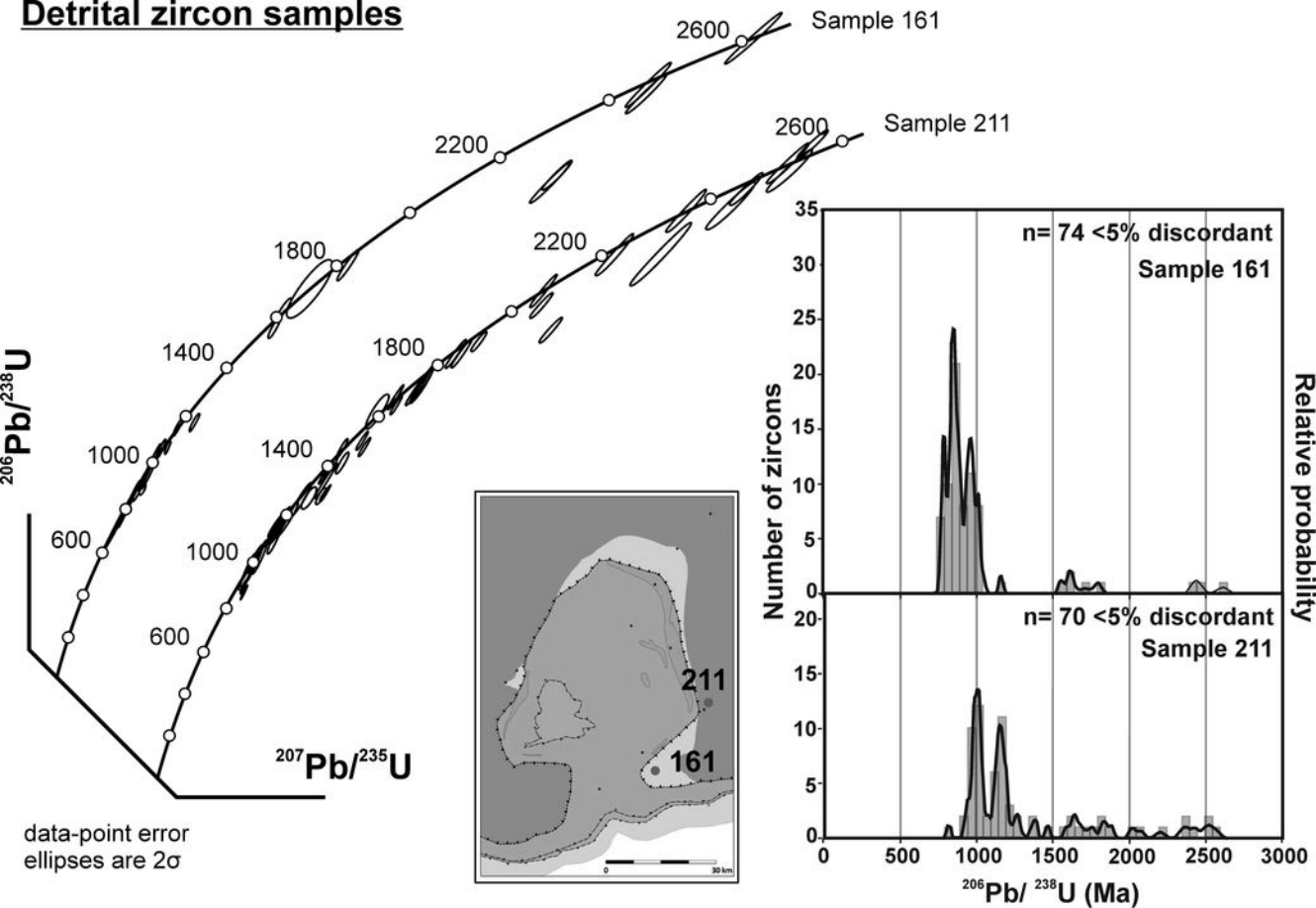
Detrital zircon samples
Sample 161
Sample 211
2600
2200
1800
1400
1000
600
$^{206}Pb/^{238}U$
$^{207}Pb/^{235}U$
data-point error
ellipses are 2σ
211
161
n= 74 <5% discordant
Sample 161
n= 70 <5% discordant
Sample 211
Number of zircons
Relative probability
0
5
10
15
20
25
30
35
500
1000
1500
2000
2500
3000
$^{206}Pb/^{238}U$ (Ma)

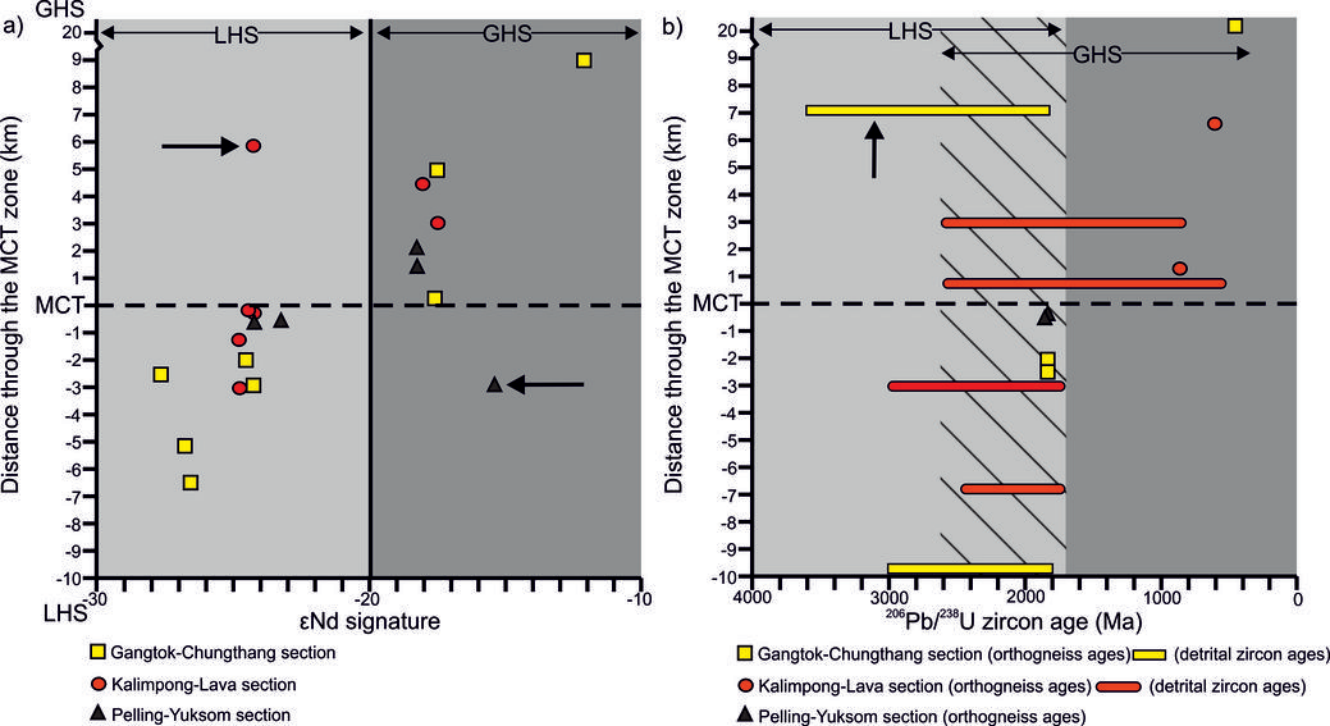
a)
GHS
LHS
GHS
Distance through the MCT zone (km)
MCT
LHS
-30
-20
-10
εNd signature
b)
LHS
GHS
Distance through the MCT zone (km)
MCT
4000
3000
2000
1000
0
$^{206}Pb/^{238}U$ zircon age (Ma)
Gangtok-Chungthang section
Kalimpong-Lava section
Pelling-Yuksom section
Gangtok-Chungthang section (orthogneiss ages)
(detrital zircon ages)
Kalimpong-Lava section (orthogneiss ages)
(detrital zircon ages)
Pelling-Yuksom section (orthogneiss ages)

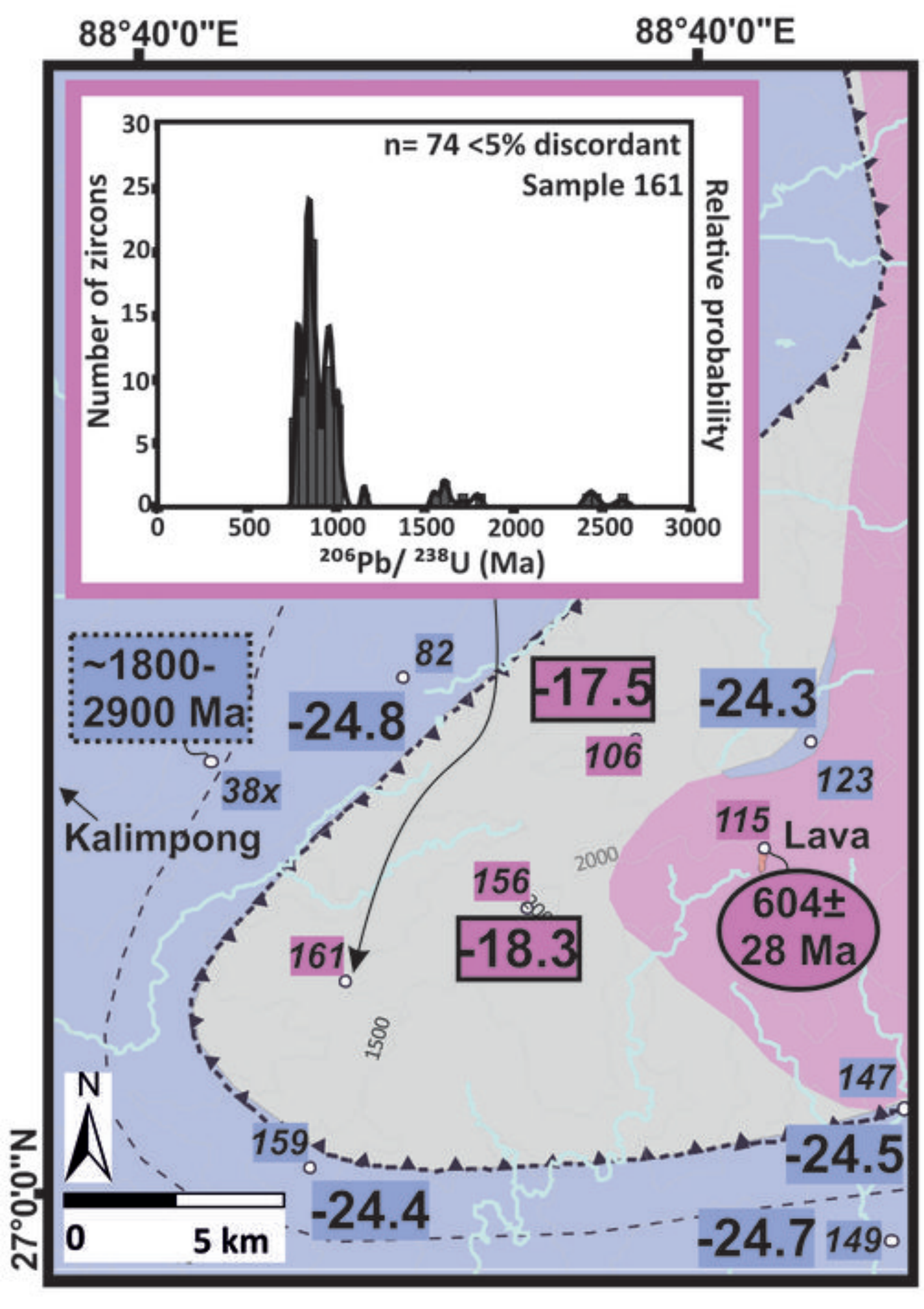
88°40'0"E
88°40'0"E
27°0'0"N
n= 74 <5% discordant
Sample 161
Number of zircons
Relative probability
30
25
20
15
10
5
0
0
500
1000
1500
2000
2500
3000
206Pb/ 238U (Ma)
~1800-
2900 Ma
82
-24.8
-17.5
-24.3
106
123
38x
Kalimpong
115
Lava
2000
156
604±
28 Ma
161
-18.3
1500
147
N
159
-24.5
-24.4
-24.7
149
0
5 km

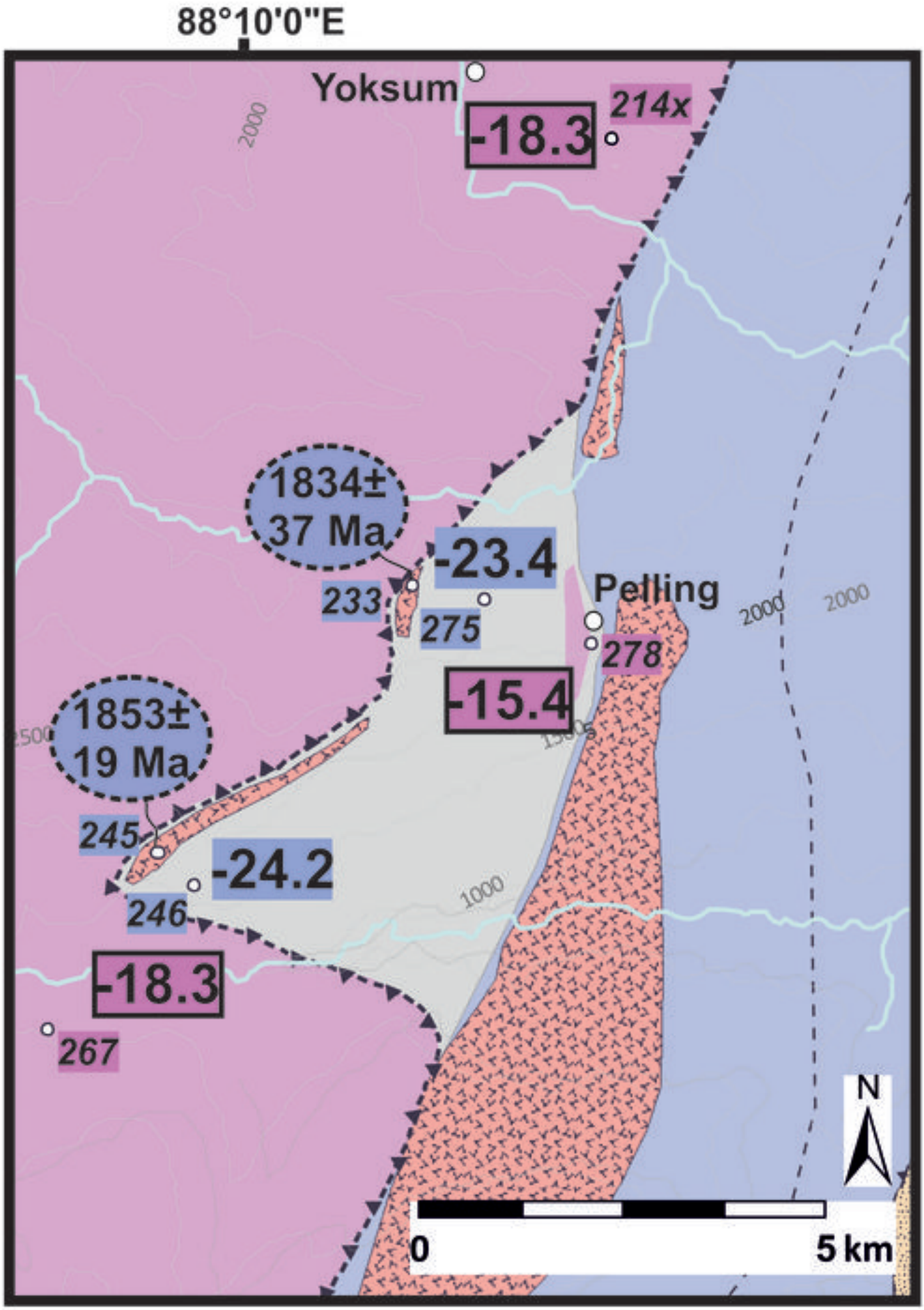
88°10'0"E
Yoksum
214x
-18.3
2000
1834±
37 Ma
-23.4
233
275
Pelling
278
2000
2000
-15.4
1853±
19 Ma
245
-24.2
246
1000
-18.3
267
N
0
5 km

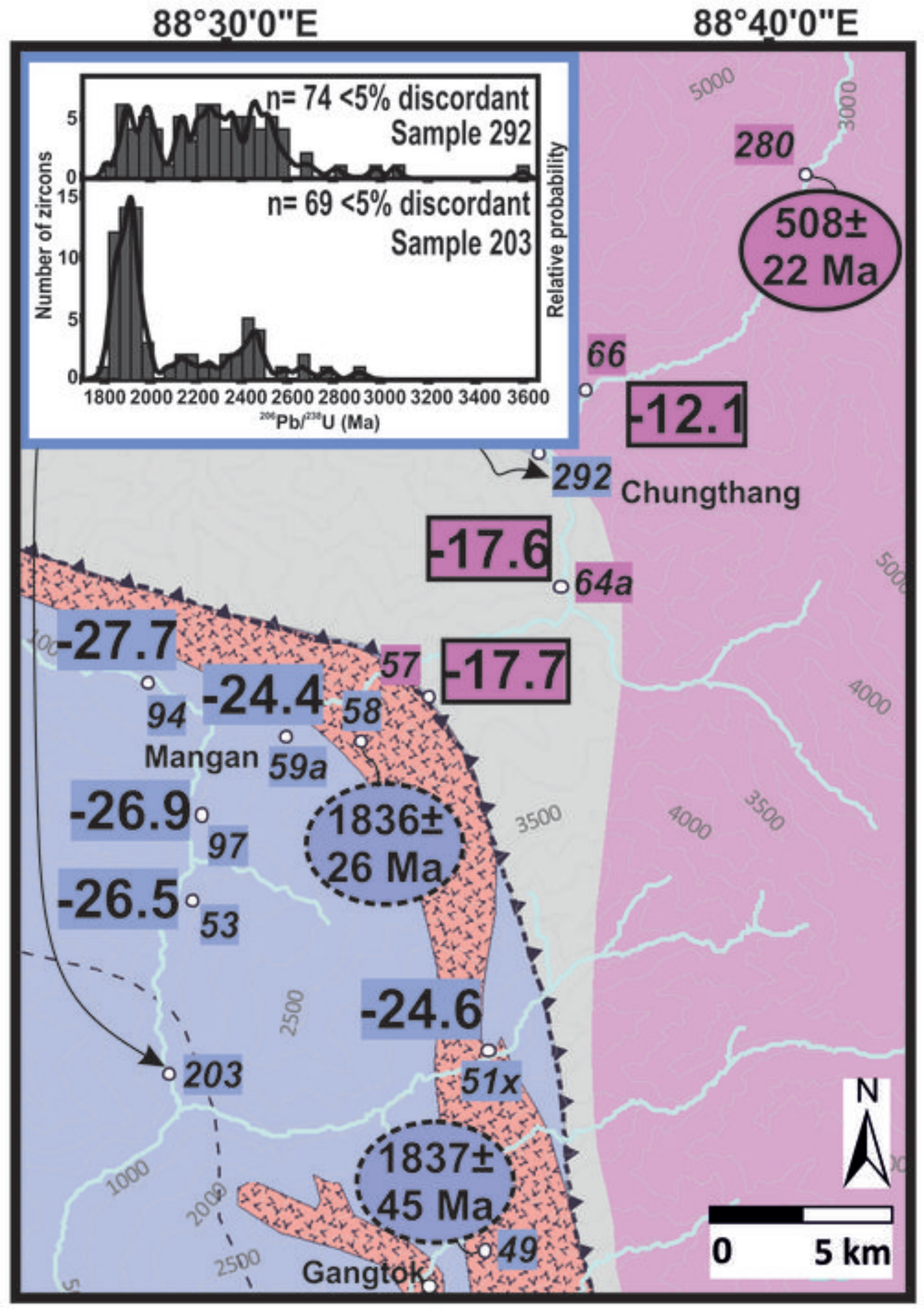
88°30'0"E
88°40'0"E
n= 74 <5% discordant
Sample 292
n= 69 <5% discordant
Sample 203
Number of zircons
Relative probability
1800 2000 2200 2400 2600 2800 3000 3200 3400 3600
206Pb/238U (Ma)
280
508± 22 Ma
66
-12.1
292
Chungthang
-17.6
64a
-27.7
57
-17.7
-24.4
58
94
Mangan
59a
-26.9
97
1836± 26 Ma
-26.5
53
-24.6
203
51x
1837± 45 Ma
49
Gangtok
5000
3000
4000
3500
2500
1000
2000
N
0
5 km

Mid-Palaeozoic architecture

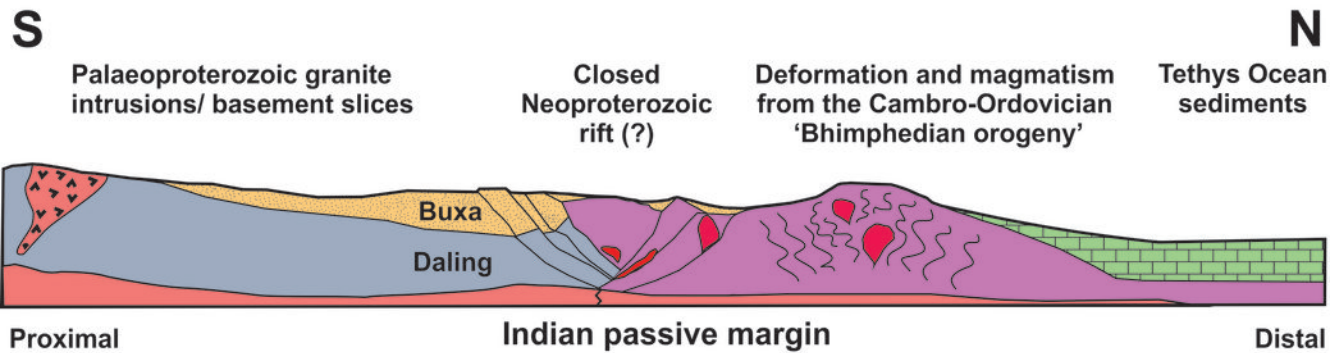

Schematic (not to scale)